SAND2014-1582C

Exceptional service in the national interest

Sandia National Laboratories

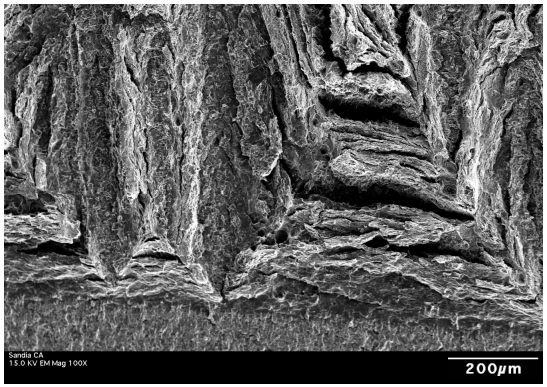

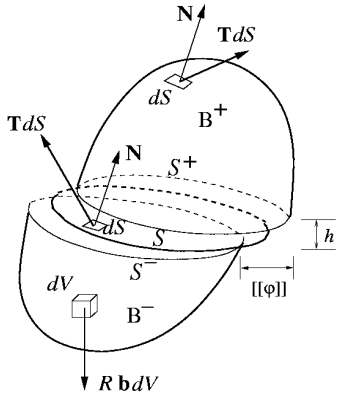

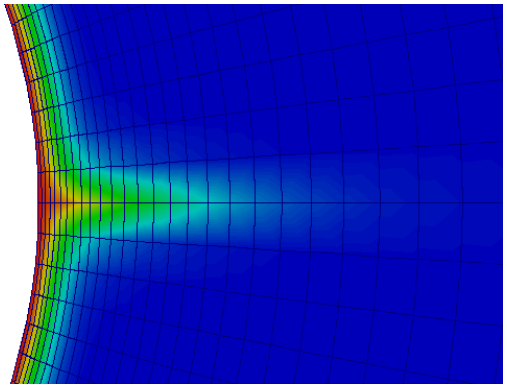

Simulating hydrogen embrittlement and fast pathways for diffusion through localization elements

J. Foulk III, W. Sun, J. Ostien, A. Mota, C. San Marchi, B. Somerday

ME Seminar 395 Seminar Series, Stanford University

February 27, 2014

U.S. DEPARTMENT OF ENERGY | NNSA Nuclear National Security Administration

Sandia National Laboratories is a multi-program laboratory managed and operated by Sandia Corporation, a wholly owned subsidiary of Lockheed Martin Corporation, for the U.S. Department of Energy's National Nuclear Security Administration under contract DE-AC04-94AL85000. SAND NO. 2011-XXXXP

The driving force and the resistance

Sandia National Laboratories

Π – potential energy of body
R – resistance of the body
a - crack length

$$\frac{\partial \Pi}{\partial a} + R(a) = 0$$

energetics of crack propagation

calculate driving forces

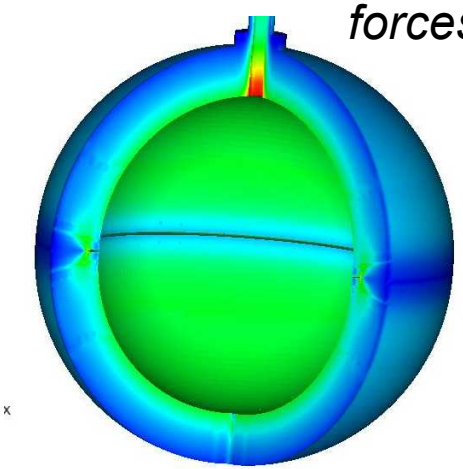

$$J = \int_{\Gamma_0} \boldsymbol{L} \cdot \boldsymbol{\Sigma} \boldsymbol{N} dA$$

L – crack trajectory
Σ – Energy-momentum tensor
N – surface normal

measure fracture toughness

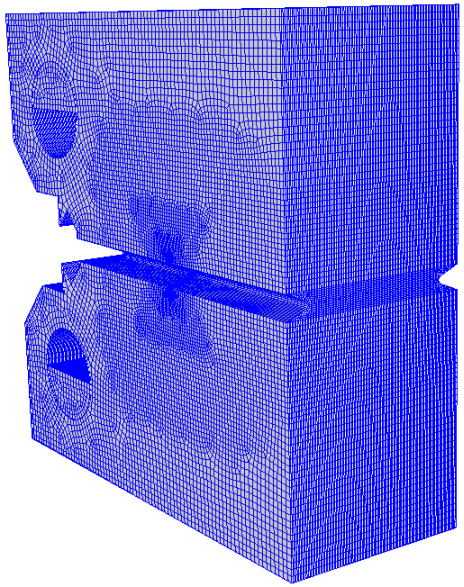

quantify fracture mechanisms

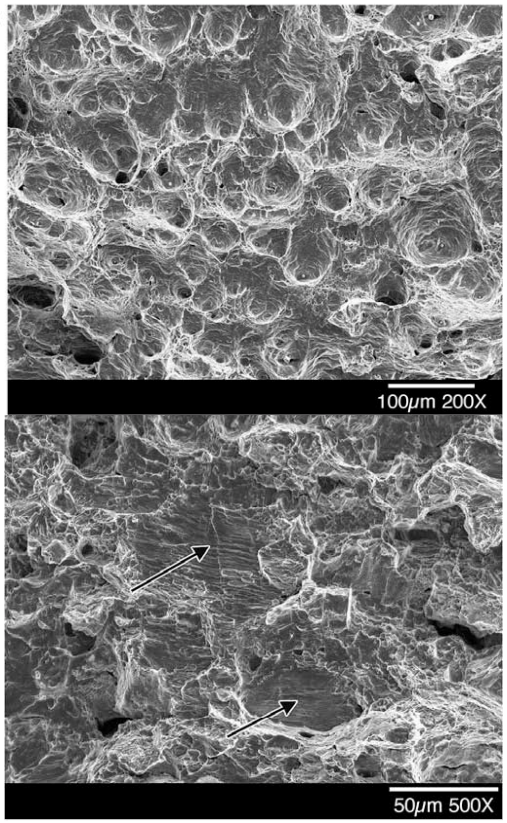

Our goal is to model the resistance and predict crack initiation and propagation

Hydrogen localizes deformation

The role of localized deformation in hydrogen-assisted crack propagation in 21Cr-6Ni-9Mn stainless steel, Nibur, Somerday, Balch, and San Marchi, Acta Materialia, 2009.

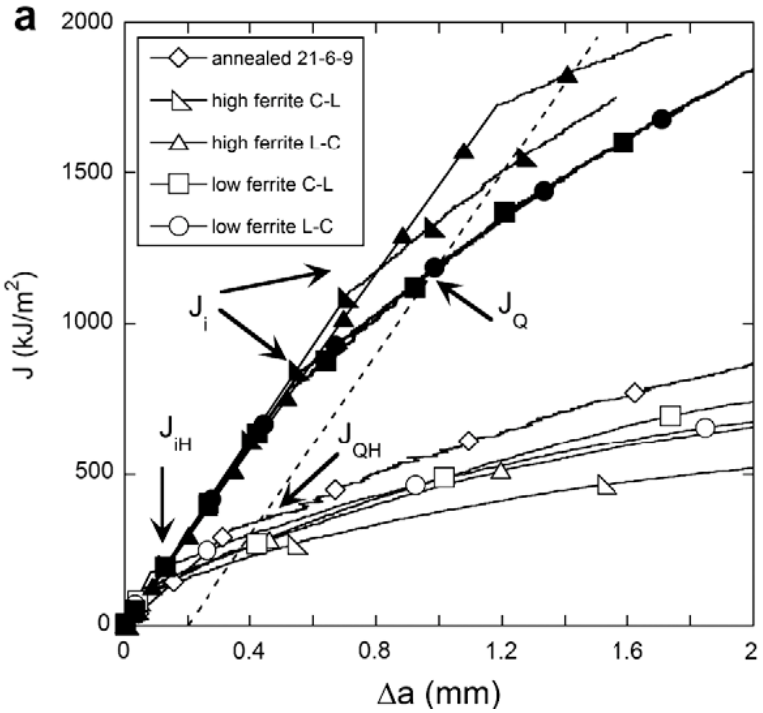

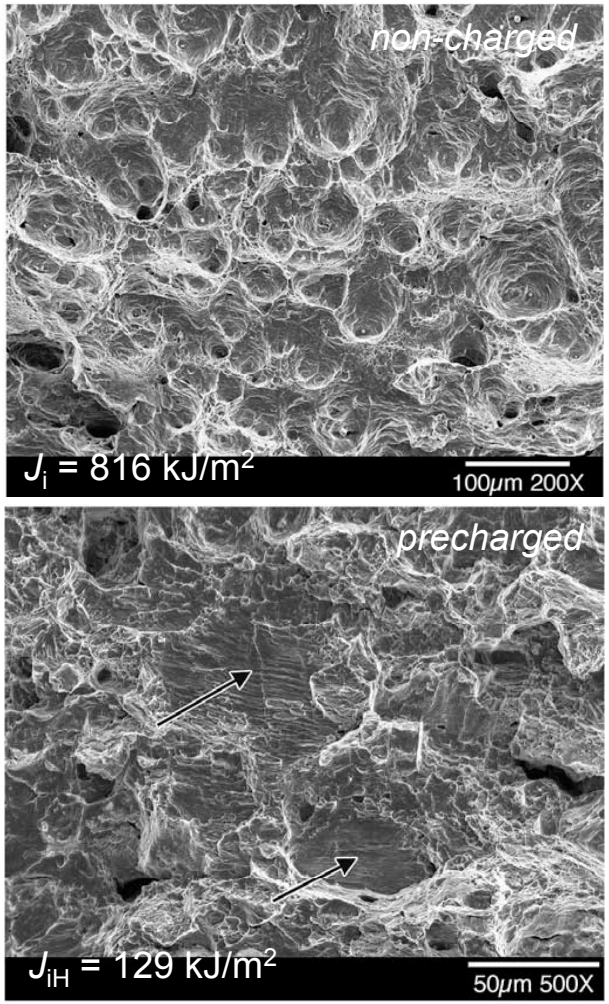

forged, low ferrite, 21-6-9 (L-C)

- Hydrogen enhanced localized deformation (HELP)
  - Increases dislocation mobility
  - Stabilized edge component
  - Deformation bands (slip localization) evolve
- Voids nucleate at intersection of boundaries
- Planar nucleation and growth – elongated dimples

Embrittlement stems from hydrogen enhanced localized deformation – Coupling needed!

Initial studies in 21Cr-6Ni-9Mn SS

- Compact tension specimens, B ~ 13 mm; W ~ 26 mm
- Constant pressure of gaseous hydrogen: 103 MPa
- "Loading rates" ~ 0.6 - 10 MPa $m^{1/2}$ per minute

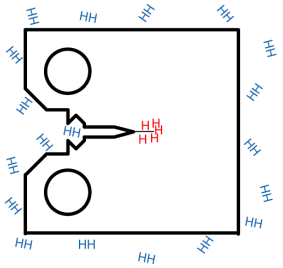

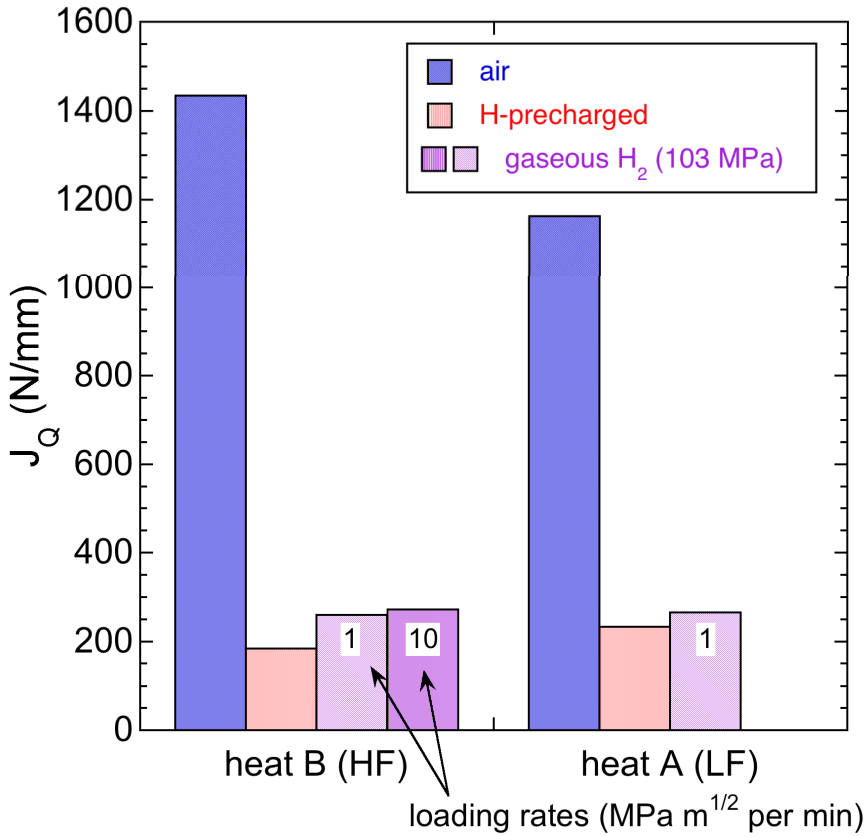

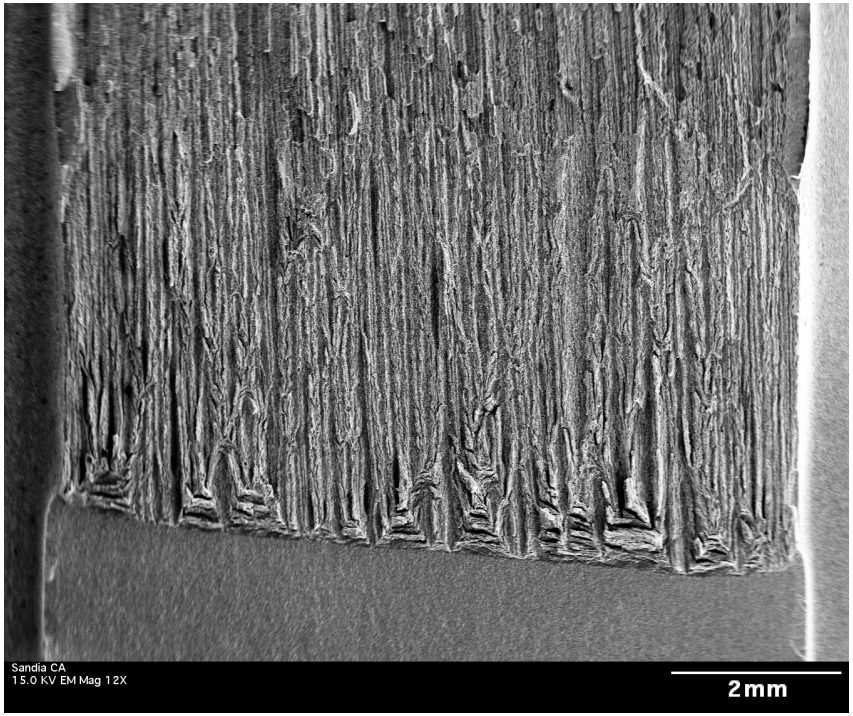

Note: 220 MPa $m^{1/2}$ = 224 kJ/m^2 (N/mm)

Rapid crack growth in 21Cr-6Ni-9Mn

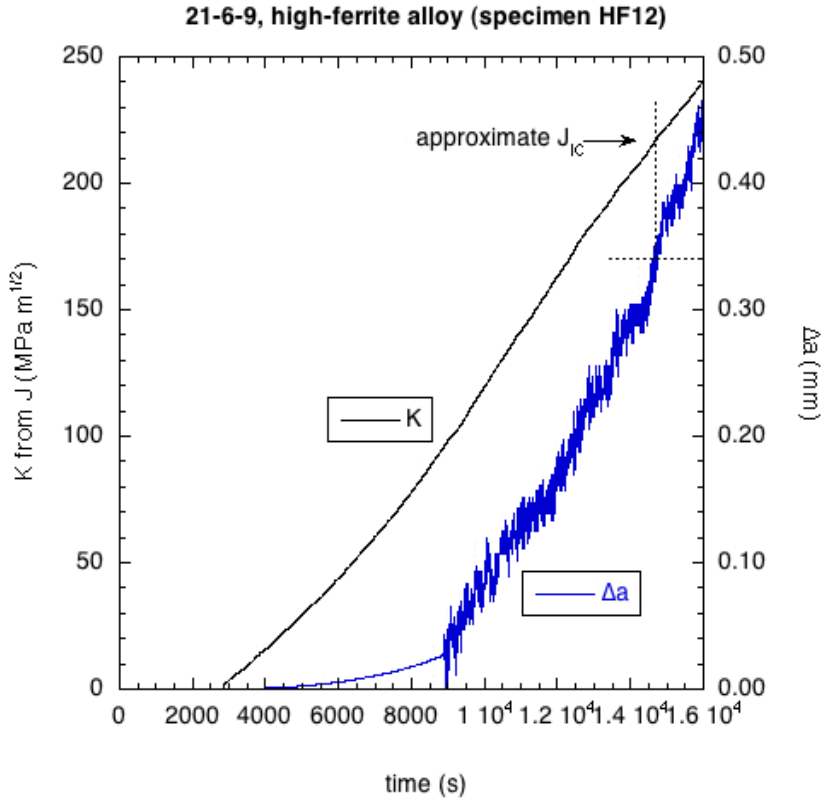

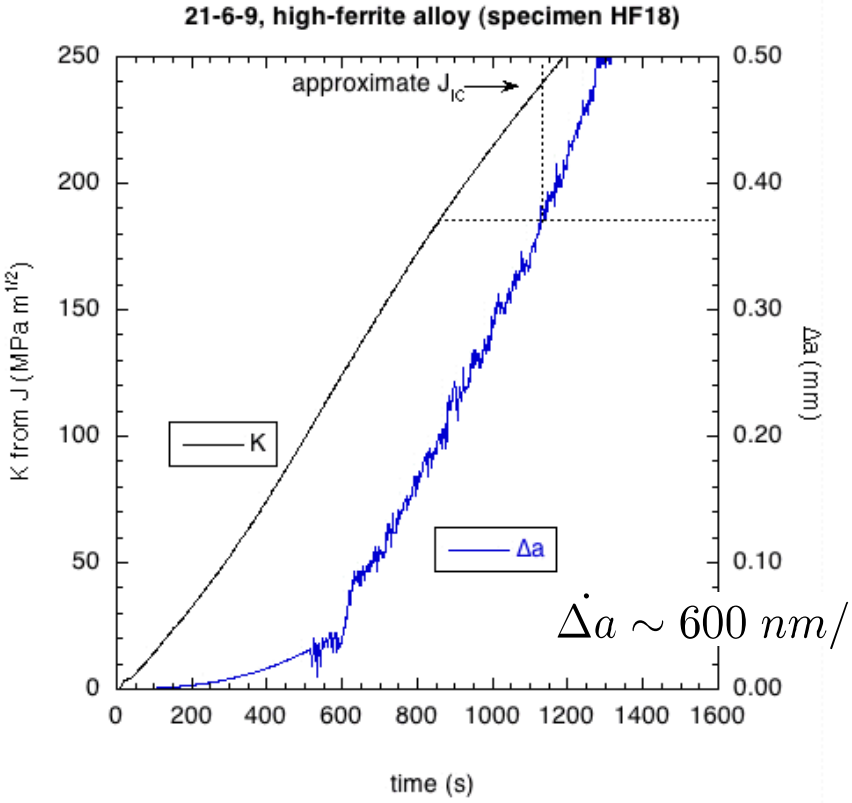

$\dot{\Delta a} \sim 600\ nm/s$

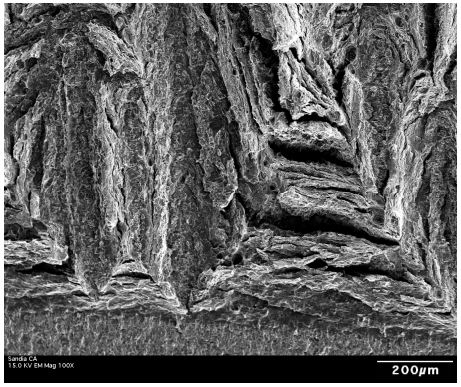

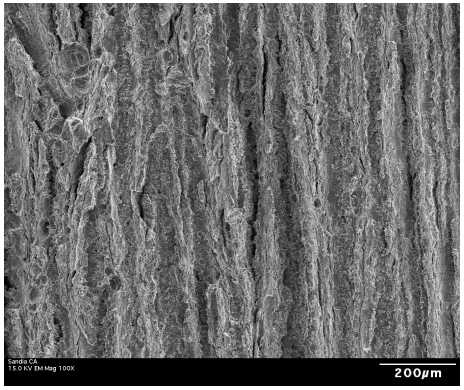

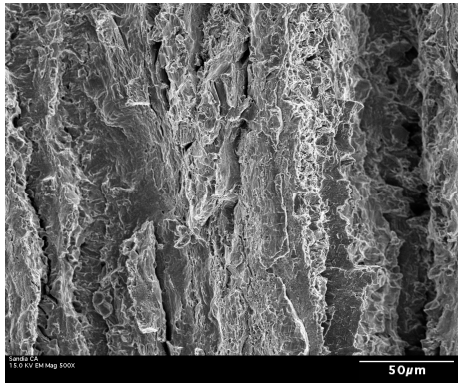

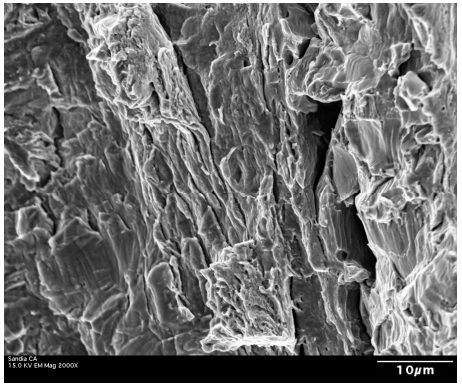

(HF18)

Modeling 21Cr-6Ni-9Mn in H_2 gas

Before moving to complex and computationally challenging fracture geometries, we need to understand phenomena in plane strain

Mechanical analysis should be performed to help experimentalists reduce driving forces from non-standard fracture geometry. Iteration required.

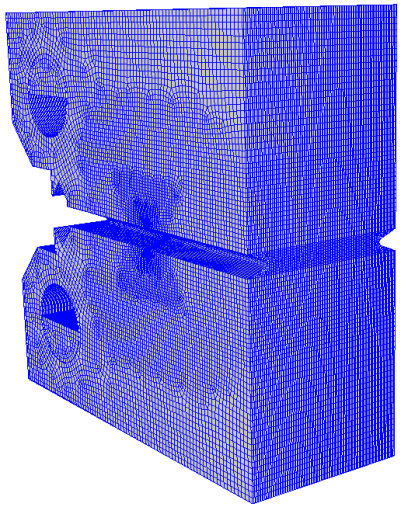

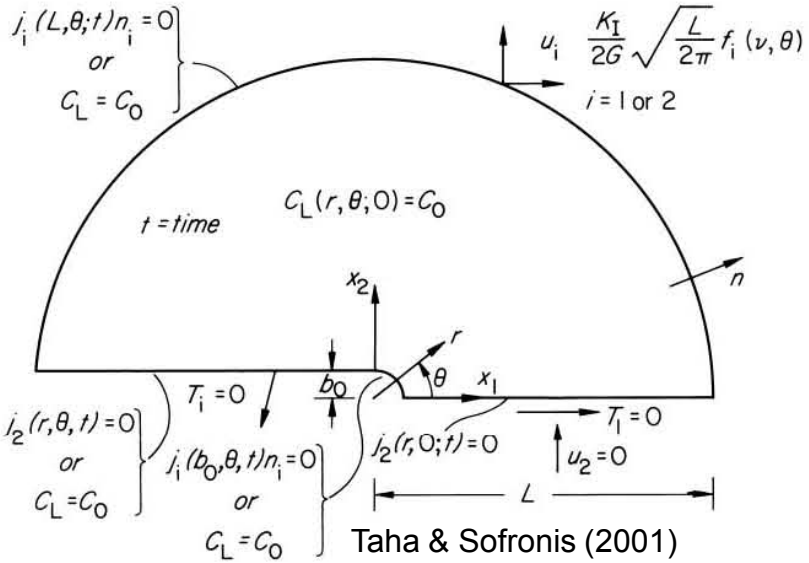

Taha & Sofronis (2001)

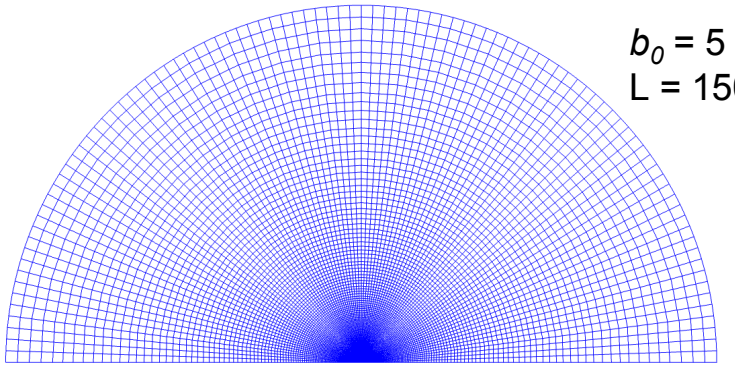

b_0 = 5 μm
L = 150 mm

nodes: 189,312
h: 40 nm x 200 nm

NOTE: Not pre-charged, constant concentration $C_{L,applied}$ applied to crack faces

Coupled hydrogen transport

This path heavily leverages Sofronis/McMeeking (1989)* and Krom (1998).
Recent work by Leo and Anand (2013).

chemical potential

$$\mu_l = \mu_0 + RT\ln(\theta_l) - v_h\sigma_h$$

model for flux

$$\boldsymbol{j}_l = -\boldsymbol{m}_l c_l \nabla_{\boldsymbol{x}}\mu_l$$

$$\boldsymbol{F} = \frac{\partial \boldsymbol{x}}{\partial \boldsymbol{X}} \qquad J = \det[\boldsymbol{F}]$$

$$\theta_l = c_l/n_l \qquad \theta_t = c_t/n_t$$

$$n_l = N_L/J \qquad n_t = N_T(\epsilon_p)/J$$

$$v_h = V_H J \qquad \tau_h = J\sigma_h$$

$$\boldsymbol{d}_l = RT\boldsymbol{m}_l$$

conservation of hydrogen

$$\frac{d}{dt}\int_B c dv = -\int_{\partial B}\boldsymbol{j}\cdot\boldsymbol{n}da \qquad \dot{c} = \dot{c}_l + \frac{\partial c_t}{\partial cl}\dot{c}_l + \frac{\partial c_t}{\partial n_t}\frac{\partial n_t}{\partial \epsilon_p}\dot{\epsilon}_p + \frac{\partial c_t}{\partial n_t}\frac{\partial n_t}{\partial J}\dot{J}$$

$$c_t = c_t(c_l, \epsilon_p, J)$$

equilibrium of lattice/trap sites

$$\theta_t = \frac{1}{1+\frac{1}{k_t\theta_l}} \qquad C^* = c_l + \frac{n_t}{1+\frac{n_l}{k_t c_l}} \qquad D^* = 1 + \frac{\partial c_t}{\partial c_l}$$

$$D^*\dot{c}_l + C^*\mathrm{div}\boldsymbol{v} - \nabla_{\boldsymbol{x}}\cdot\boldsymbol{d}_l\nabla_{\boldsymbol{x}}c_l - \nabla_{\boldsymbol{x}}\cdot\frac{c_l}{J}\boldsymbol{d}_l\nabla_{\boldsymbol{x}}J + \nabla_{\boldsymbol{x}}\cdot\frac{c_l V_H}{RT}\boldsymbol{d}_l\nabla_{\boldsymbol{x}}\tau_h +$$

$$\frac{\theta_l}{J}\frac{\partial N_T}{\partial \epsilon_p}\dot{\epsilon}_p - \frac{\theta_t N_T}{J^2}\dot{J} = 0$$

*P. Sofronis and R.M. McMeeking, J. Mech. Phys. Solids 37 (1989) 317

Simplification in reference

Transport of hydrogen in the current configuration

$$D^*\dot{c}_l + C^*\mathrm{div}\boldsymbol{v} - \nabla_{\boldsymbol{x}}\cdot\boldsymbol{d}_l\nabla_{\boldsymbol{x}}c_l - \nabla_{\boldsymbol{x}}\cdot\frac{c_l}{J}\boldsymbol{d}_l\nabla_{\boldsymbol{x}}J + \nabla_{\boldsymbol{x}}\cdot\frac{c_l V_H}{RT}\boldsymbol{d}_l\nabla_{\boldsymbol{x}}\tau_h + \frac{\theta_l}{J}\frac{\partial N_T}{\partial\epsilon_p}\dot{\epsilon}_p - \frac{\theta_t N_T}{J^2}\dot{J} = 0$$

Transport of hydrogen in the reference configuration (push back)

$$D^*\dot{C}_L - \nabla_{\boldsymbol{X}}\cdot d_l\boldsymbol{C}^{-1}\nabla_{\boldsymbol{X}}C_L + \nabla_{\boldsymbol{X}}\cdot\frac{d_l V_H}{RT}\boldsymbol{C}^{-1}\nabla_{\boldsymbol{X}}\tau_h C_L + \theta_T\frac{dN_T}{d\epsilon_p}\dot{\epsilon}_p$$

transient term

diffusion term

advection term from pressure

source term from trapping

Deformation-dependent diffusivity $\boldsymbol{D}_L = \boldsymbol{F}^{-1}\boldsymbol{d}_l\boldsymbol{F}^{-T} = d_l\boldsymbol{C}^{-1}$

Baseline properties for 21Cr-6Ni-9Mn

*Transport**

D_0 = 5.4E-7 m^2/s

Q = 53.9E3 J/mol

R = 8.314 J/(mol K)

T = 300 K

D_L = 2.2E-16 m^2/s

N_A = 6.0232 atoms/mol

V_M = 7.116E-6 m^3/mol – molar volume of Fe

V_H = 2.0E-6 m^3/mol – partial molar volume of H

N_L = 8.46E28 atoms/m^3 = 1.40E5 solvent lattice mol/m^3

$C_{L,0}$ = 38.7 mol/m^3 (from 316 alloys, assumes 5 wppm)

$C_{L,applied}$ = 560 mol H/m^3 (280 moles H_2/m^3)

$N_{T,total} = \alpha N_T = 10N_T = 10^{(26.6 - 1.5\exp(-6.96ep))}$ mole/m^3

$C_{T,0}$ = 3.94E24 atoms/m^3 = 6.542 mol/m^3

W_B = 9.65E3 J/mol

K_T = 47.9

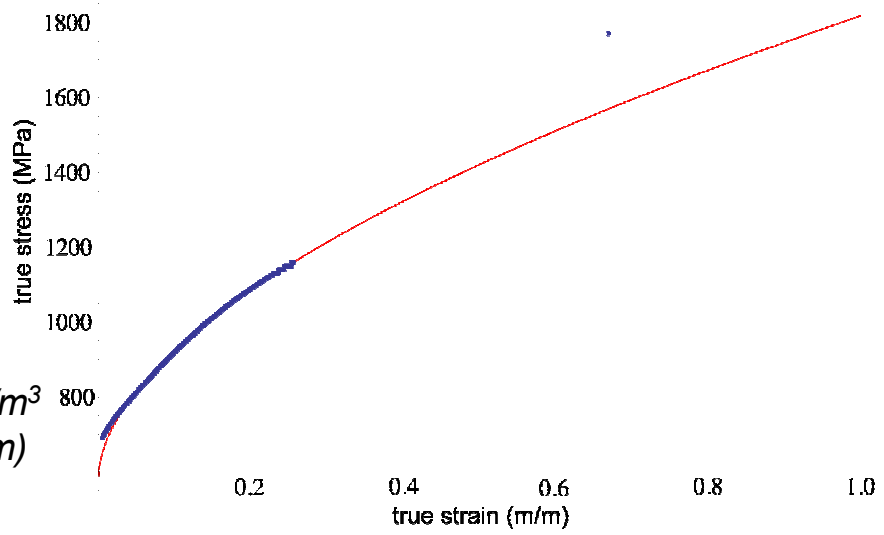

$$C_{L,applied} = K f^{\frac{1}{2}}$$ San Marchi, et al., IJHE, 2007

Mechanics – non-charged, forged, transverse, LF

ρ = 7806 kg/m^3

E = 196.6 GPa

ν = 0.3

σ_0 = 590 MPa

H = 1227 MPa

m = 0.563

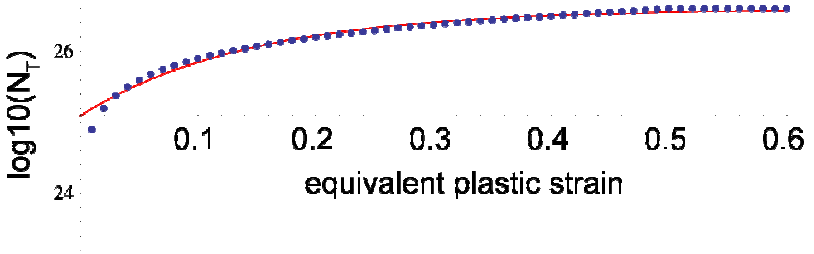

*Transport properties aligned with Somerday, et al., Met Trans, 2009

NOTE: Constant concentration, not chemical potential, is applied. Will fix.

Initial computations in 21Cr-6Ni-9Mn SS

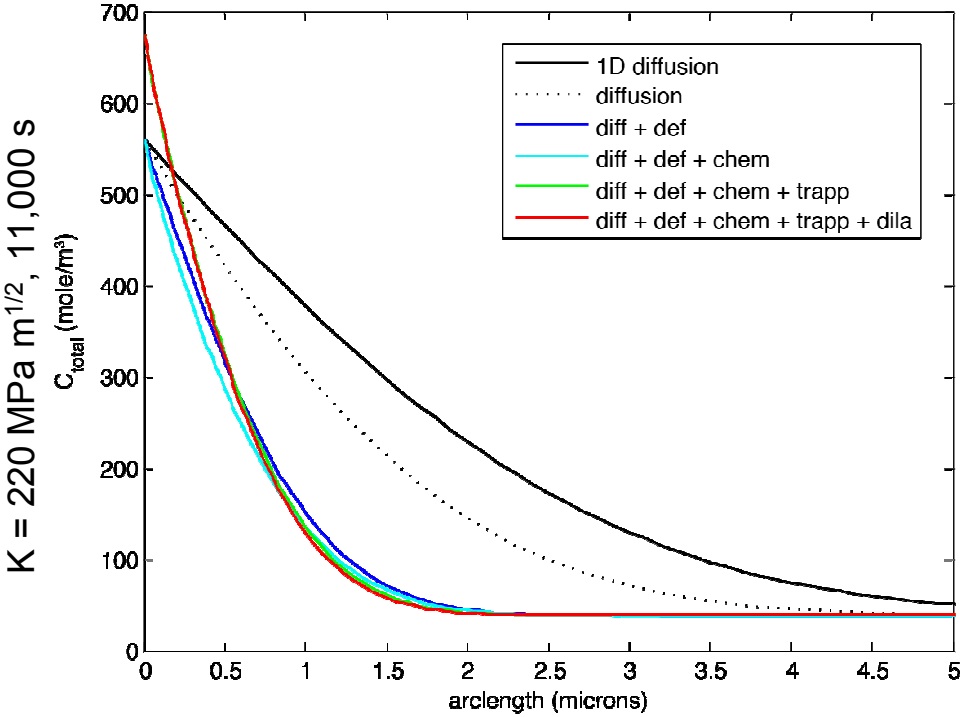

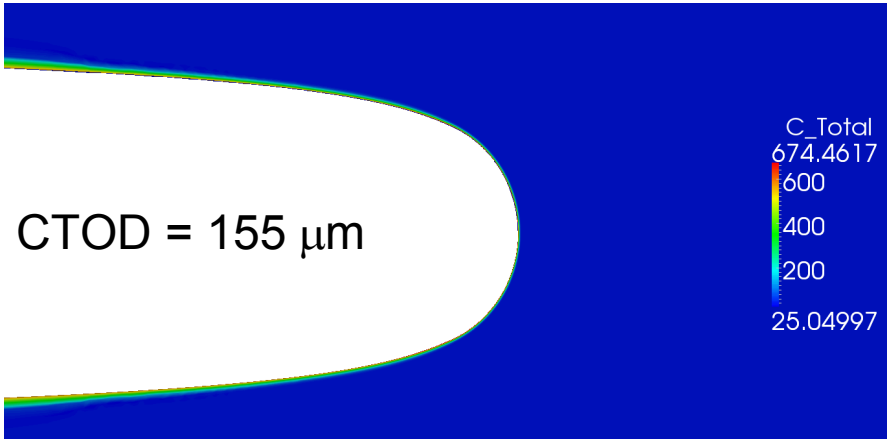

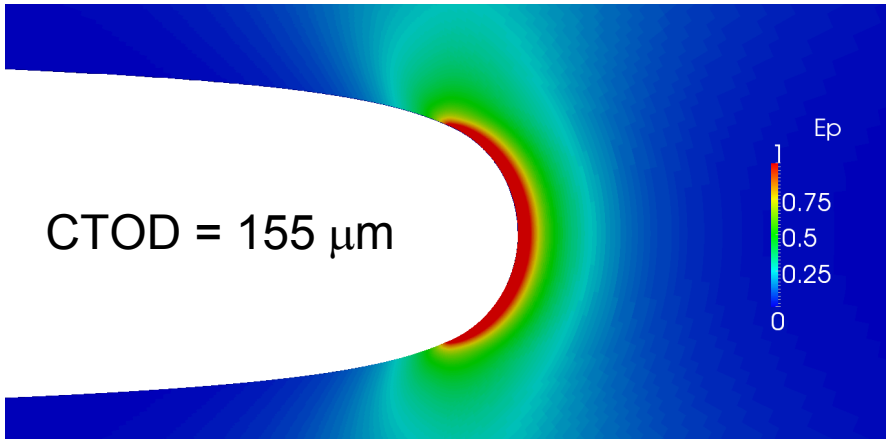

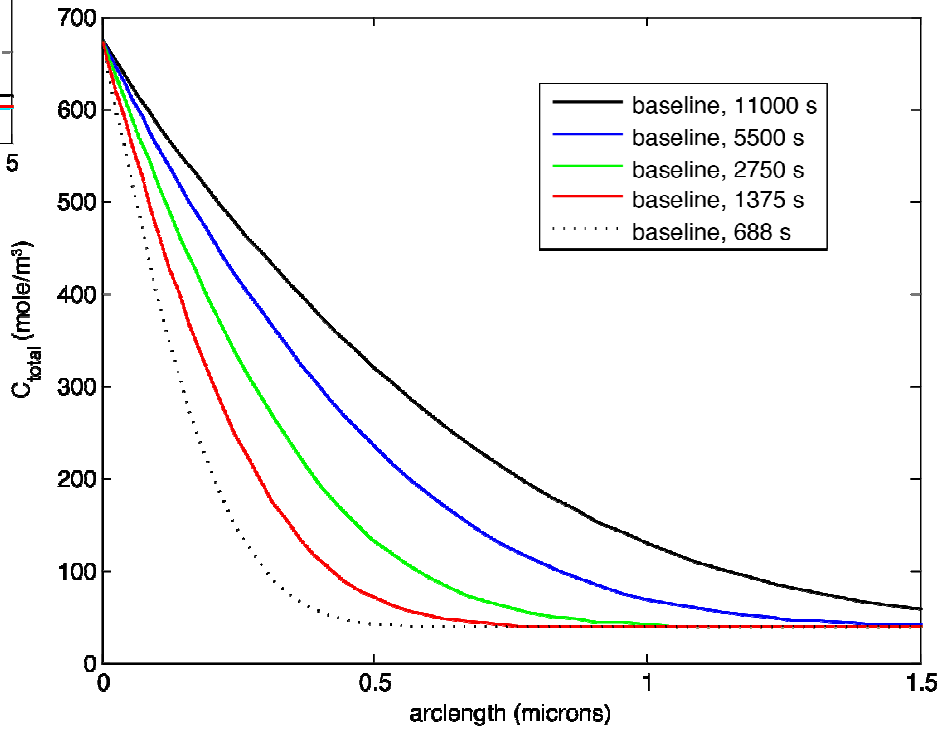

Tools useful for discovery

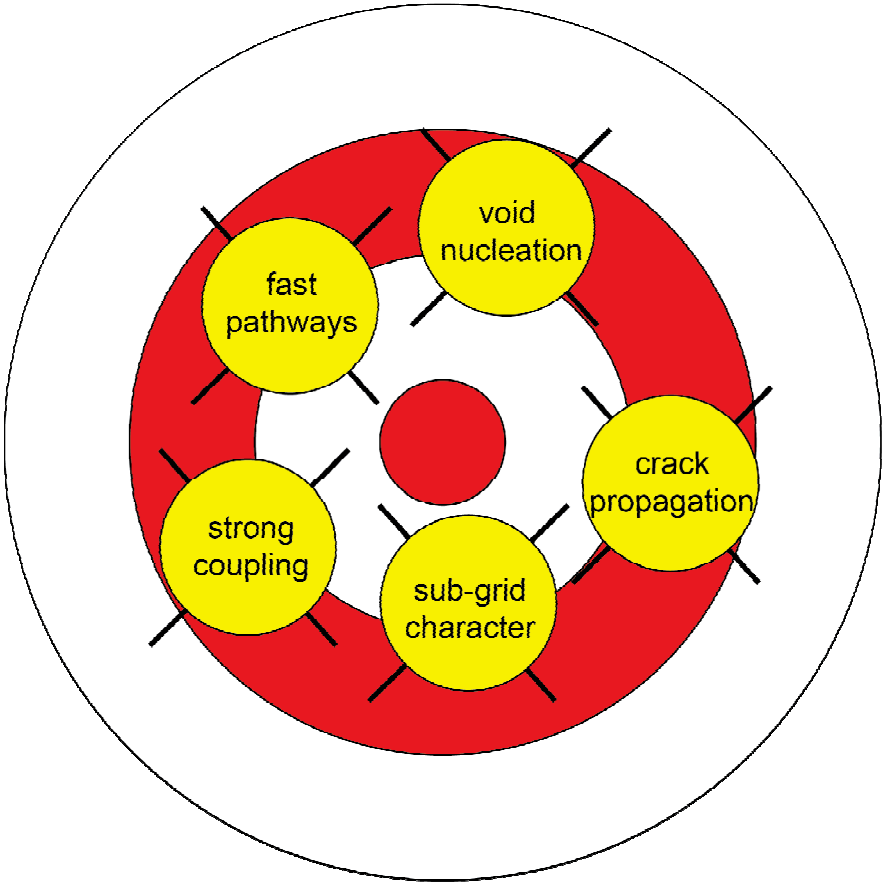

- We may need strong coupling to capture auto-catalytic processes
- Capture sub-grid processes through a smooth idealization
- Test hypotheses regarding fast pathways for diffusion
- Flexibility to easily include models for void nucleation and growth
- Model both crack initiation and propagation

Reusable Software Tool Components

Sandia National Laboratories

(Andy Salinger)

Analysis Tools (*black-box*)
- Optimization
- UQ (sampling)
- Parameter Studies
- V&V, Calibration
- OUU, Reliability

Analysis Tools (*embedded*)
- Nonlinear Solver
- Time Integration
- Continuation
- Sensitivity Analysis
- Stability Analysis
- Constrained Solves
- Optimization
- UQ Solver

Linear Algebra
- Data Structures
- Iterative Solvers
- Direct Solvers
- Eigen Solver
- Preconditioners
- Matrix Partitioning

Architecture-Dependent Kernels
- Multi-Core
- Accelerators

Composite Physics
- MultiPhysics Coupling
- System Models
- System UQ

Mesh Tools
- Mesh I/O
- Inline Meshing
- Partitioning
- Load Balancing
- Adaptivity
- Remeshing
- Grid Transfers
- Quality Improvement
- DOF map

Utilities
- Input File Parser
- Parameter List
- Memory Management
- I/O Management
- Communicators

PostProcessing
- Visualization
- Verification
- Model Reduction

Mesh Database
- Mesh Database
- Geometry Database
- Solution Database

Local Fill

Discretizations
- Discretization Library
- Field Manager

Derivative Tools
- Sensitivities
- Derivatives
- Adjoints
- UQ / PCE Propagation

Physics Fill
- Element Level Fill
- Material Models
- Objective Function
- Constraints
- Error Estimates
- MMS Source Terms

Data-Centric Algs
- Graph Algorithms
- SVDs
- Map-Reduce
- Linear Programming
- Network Models

Software Quality
- Version Control
- Regression Testing
- Build System
- Backups
- Verification Tests
- Mailing Lists
- Unit Testing
- Bug Tracking
- Performance Testing
- Code Coverage
- Porting
- Web Pages
- Release Process

LCM research environment

The Laboratory for Computational Mechanics (LCM) is a research environment that leverages Albany which employs a host reusable components in Trilinos

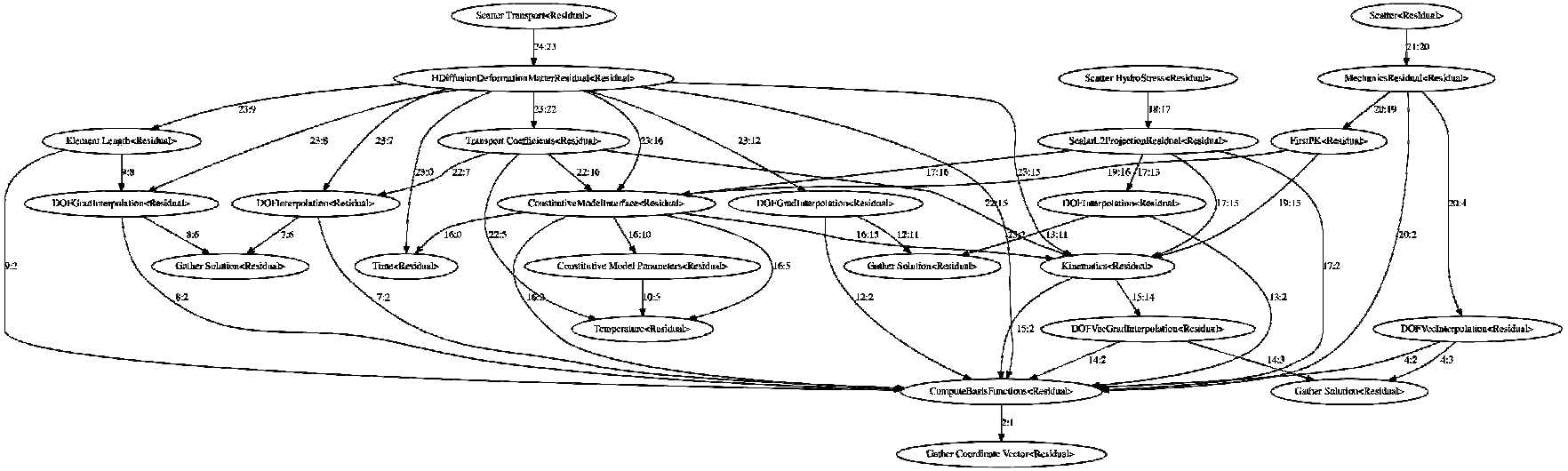

- *Phalanx* helps manage multiphysics dependencies
- *Intrepid* provides an extensive element library
- *Sacado* yields an exact Jacobian via automatic differentiation
- *NOX* provides nonlinear solution methods

https://software.sandia.gov/albany/

http://trilinos.sandia.gov/

Capture sub-grid processes

Goal: Capture sub-grid processes through methods that regularize the jump

$$\boldsymbol{F} = \boldsymbol{F}^{\parallel}\,\boldsymbol{F}^{\perp}$$

$$\boldsymbol{F}^{\parallel} = \boldsymbol{g}_i \otimes \boldsymbol{G}^i$$

$$\boldsymbol{F}^{\perp} = \boldsymbol{I} + \frac{[\![\boldsymbol{\Phi}]\!]}{h} \otimes \boldsymbol{N}$$

$$\boldsymbol{F} = \boldsymbol{F}^{\parallel} + \frac{[\![\boldsymbol{\varphi}]\!]}{h} \otimes \boldsymbol{N}$$

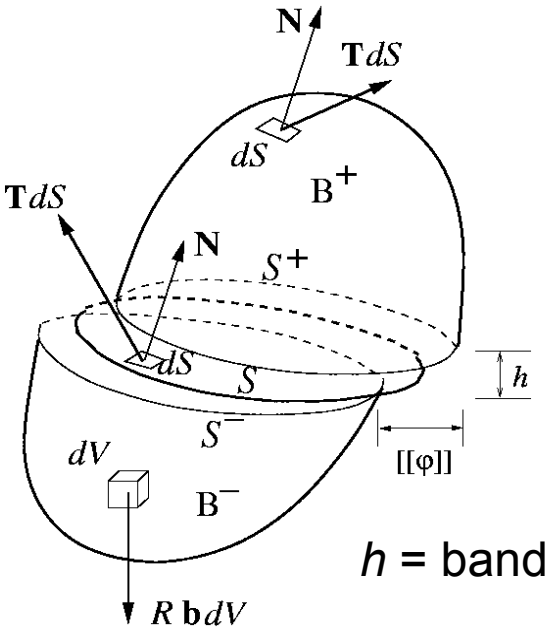

h = band thickness

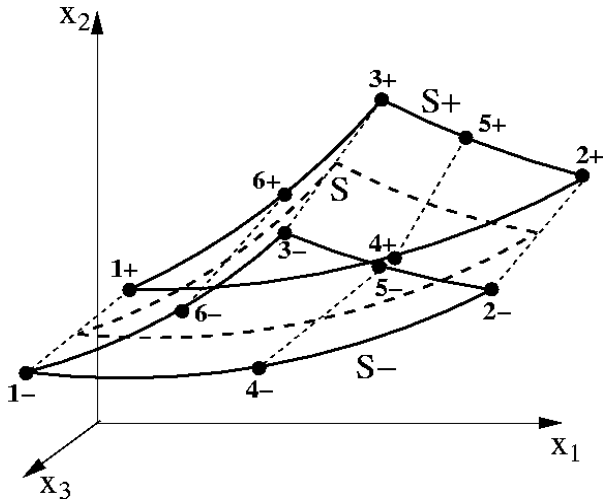

Akin to "cohesive" element

- Finite-deformation kinematics
- Simulation of strain localization
- No additional constitutive assumptions

Yang, Mota and Ortiz (IJNME, 2005), Armero and Garikipati (IJSS, 1996)

An intermediate configuration

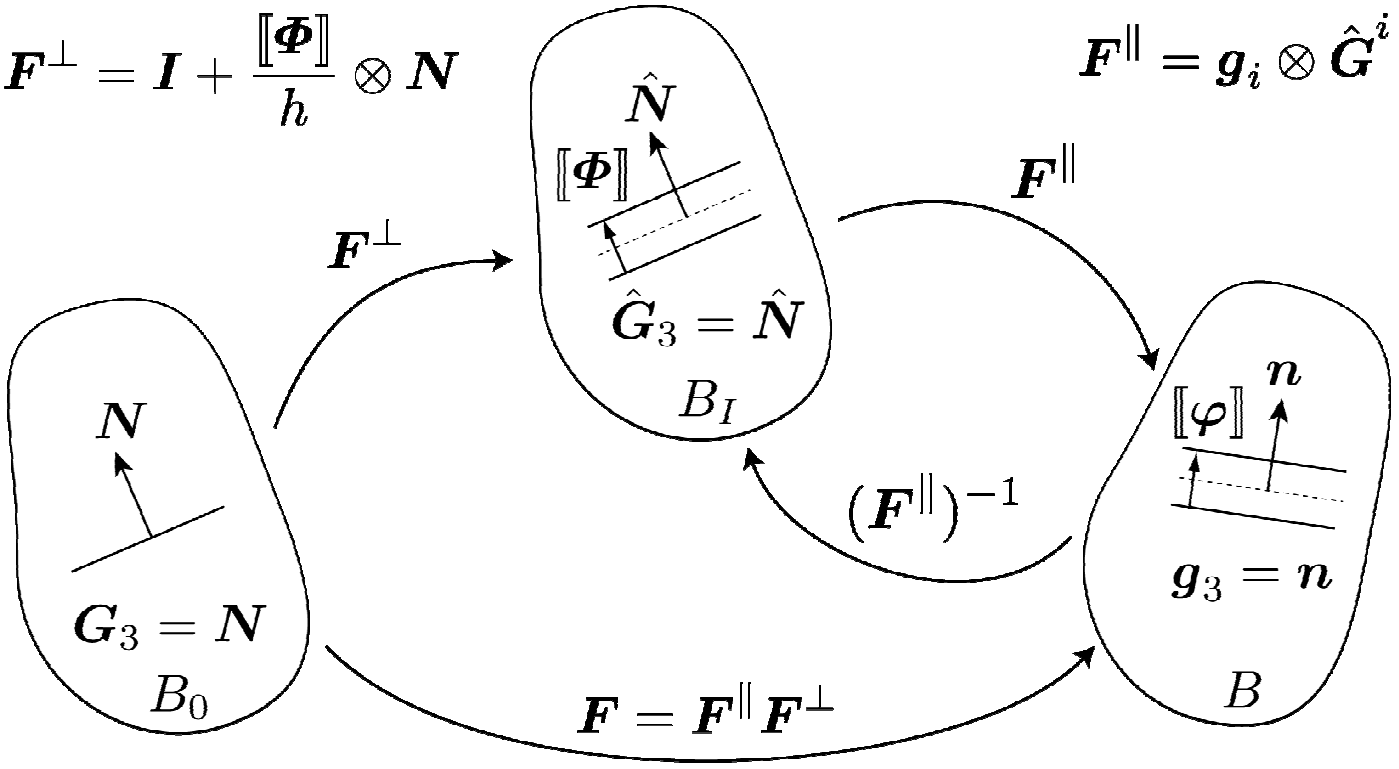

additive decomposition!

The jump is pushed backwards

$$[\![\boldsymbol{\Phi}]\!] = (\boldsymbol{F}^{\parallel})^{-1}[\![\boldsymbol{\varphi}]\!]$$

Retain definition of membrane def. grad.

$$\boldsymbol{F}^{\parallel} = \boldsymbol{g}_i \otimes \boldsymbol{G}^i$$

Damage is convergent with refinement

Sandia National Laboratories

Mesh: 02
Label: Medium
Nodes: 29,535
Elem: 23,673
s ~ 120 μm

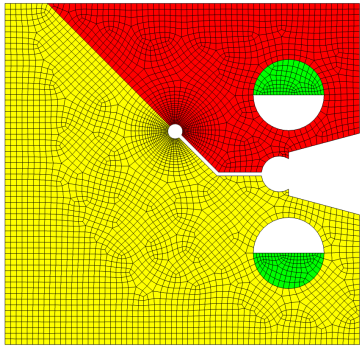

Mesh: 03
Label: Fine
Nodes: 141,831
Elem: 125,865
s ~ 60 μm

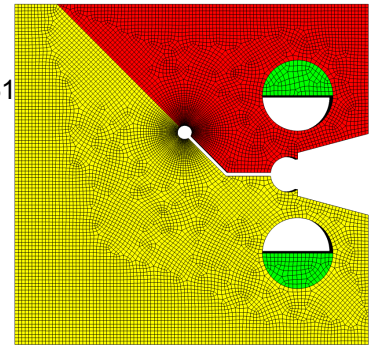

Mesh: 04
Label: Finest
Nodes: 1,079,622
Elem: 1,015,812
s ~ 30 μm

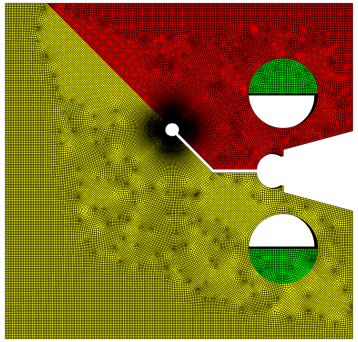

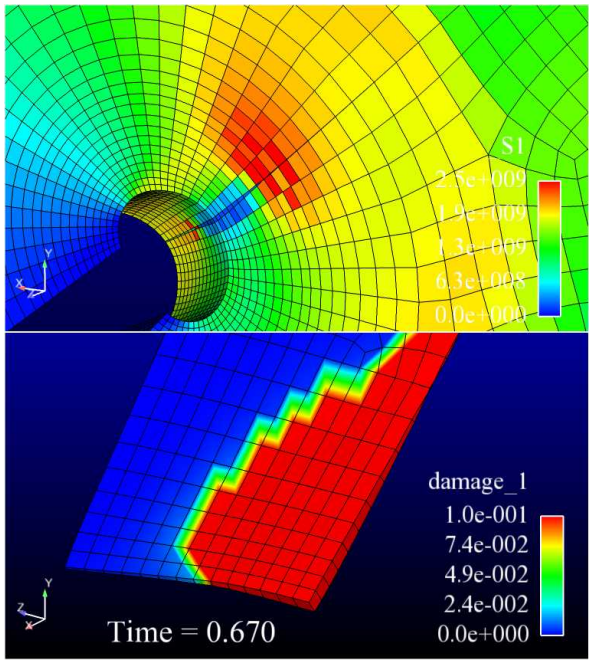

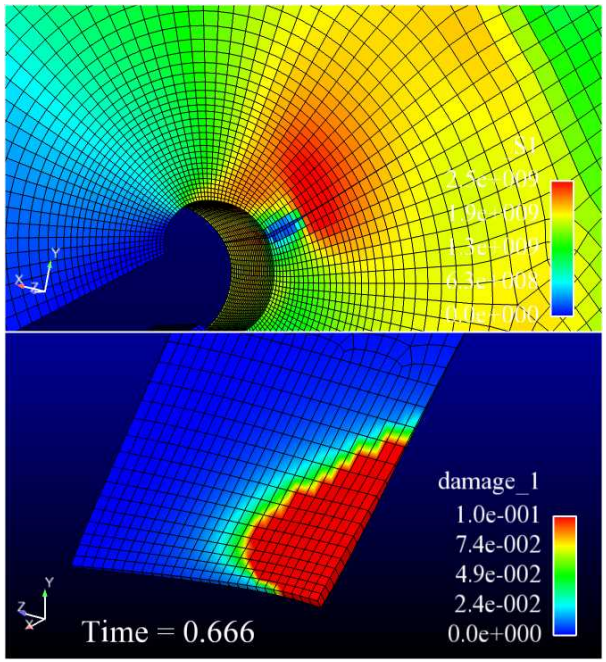

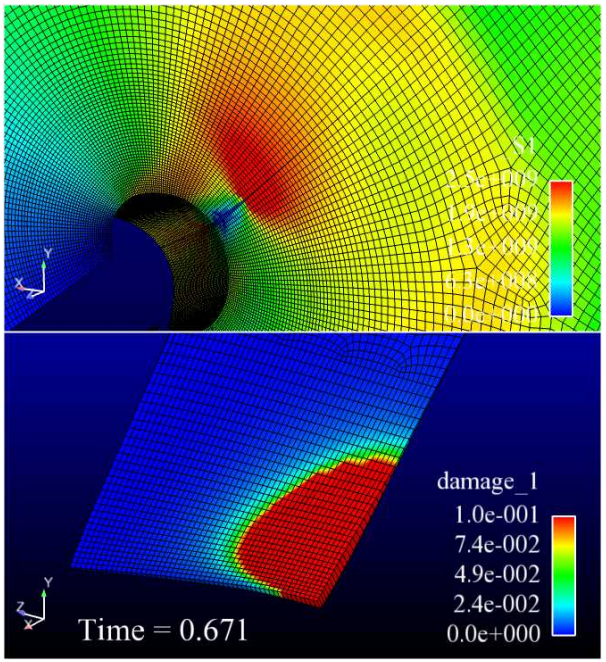

Although at slightly different times, the evolution of damage is comparable for 03 & 04.

NOTE: Smooth notch – the specimen was not pre-cracked.

Extend sub-grid model for multiphysics

Fox and Simo (1980), Callari, Armero, Abati (2010)

redefine space

$$\boldsymbol{X} = \boldsymbol{\Phi}(\xi^1, \xi^2, \xi^3) = \bar{\boldsymbol{\Phi}}(\xi^1, \xi^2) + \boldsymbol{N}(\xi^1, \xi^2)\xi^3 \qquad \boldsymbol{G}_i = \boldsymbol{\Phi}_{,i} = \frac{\partial \boldsymbol{X}}{\partial \xi^i}$$

include jump in C

$$C(\boldsymbol{X}) = \bar{C}(\boldsymbol{\phi}[\xi^1, \xi^2]) + \frac{[\![C]\!](\boldsymbol{\phi}[\xi^1, \xi^2])}{h}\xi^3 \qquad \nabla_{\boldsymbol{X}} C = (\nabla \boldsymbol{\Phi})^{-T} \frac{\partial C}{\partial \xi^i}$$

Finite element implementation is straightforward

$$\nabla_{\boldsymbol{X}} C\big|_{\xi^3=0} = [B] \begin{bmatrix} \{C\}^+ \\ \{C\}^- \end{bmatrix} = \begin{bmatrix} [B]^+ & [B]^- \end{bmatrix} \begin{bmatrix} \{C\}^+ \\ \{C\}^- \end{bmatrix}$$

$$B^{\pm}_{ia} = \begin{bmatrix} G^1_i & G^2_i & G^3_i \end{bmatrix} \cdot \begin{bmatrix} \frac{1}{2}\frac{\partial N_a}{\partial \xi^1} & \frac{1}{2}\frac{\partial N_a}{\partial \xi^2} & \pm\frac{1}{h}N_a \end{bmatrix}$$

i = # dimensions, *a* = # nodes

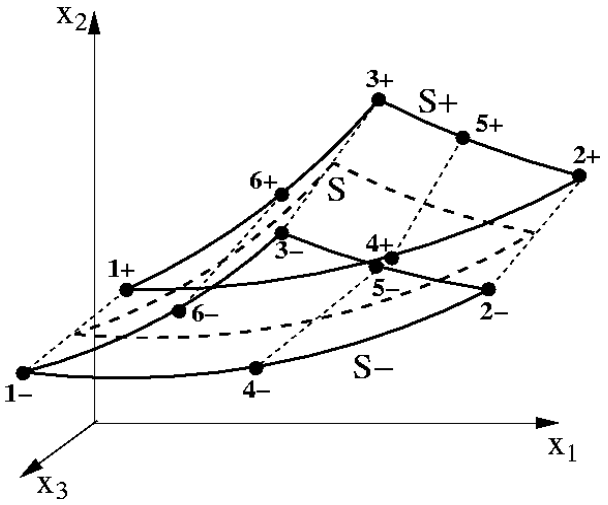

Given this gradient operator, we can use the same PDE for finite-deformation diffusion

$$D^* \dot{C}_L - \nabla_{\boldsymbol{X}} \cdot d_l \boldsymbol{C}^{-1} \nabla_{\boldsymbol{X}} C_L + \nabla_{\boldsymbol{X}} \cdot \frac{d_l V_H}{RT} \boldsymbol{C}^{-1} \nabla_{\boldsymbol{X}} \tau_h C_L + \theta_T \frac{dN_T}{d\epsilon_p} \dot{\epsilon}_p$$

Examining a fast pathway

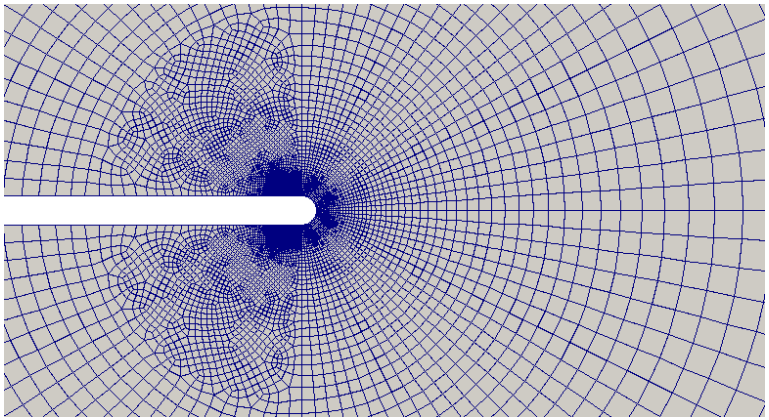

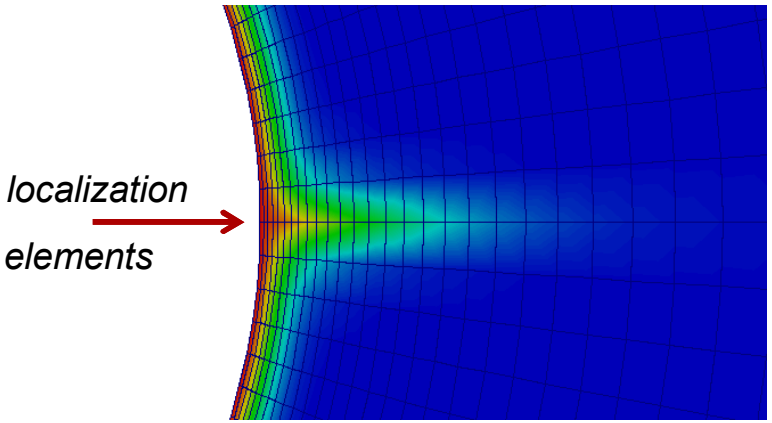

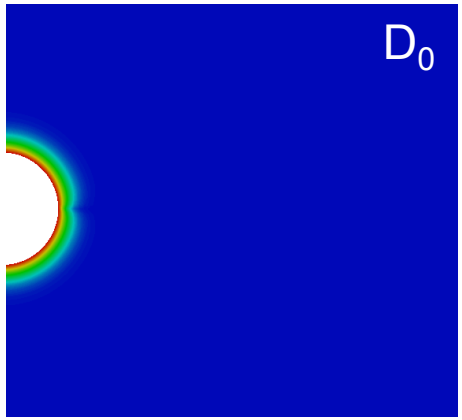

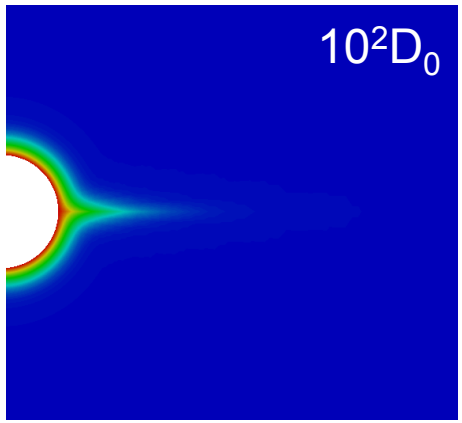

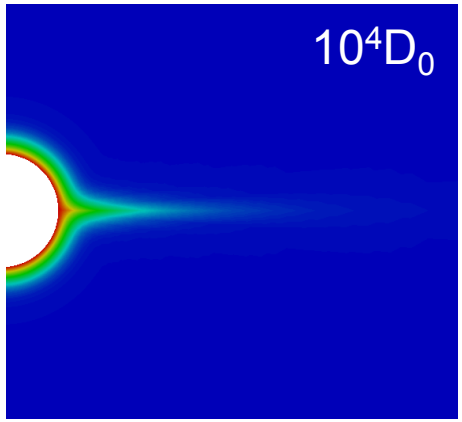

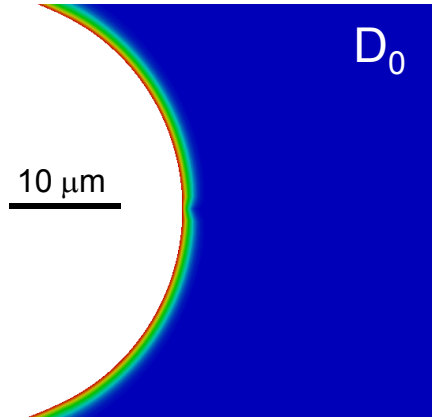

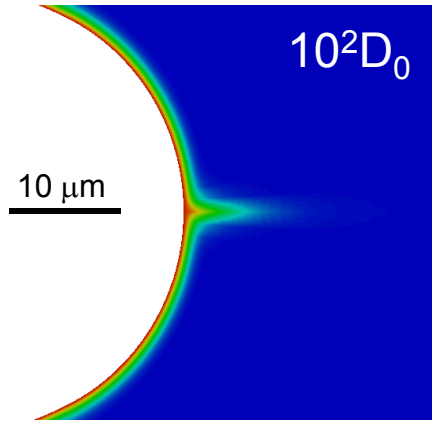

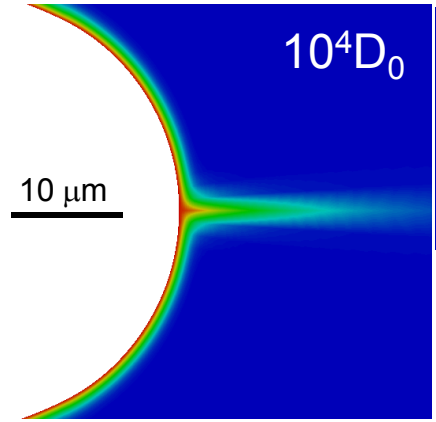

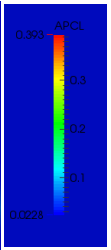

- Baseline properties, 21-6-9
- Study: D_0, 10^2D_0 , 10^4D_0
- No deformation, 100 MPa $m^{1/2}$
- Rate: 100 MPa $m^{1/2}$ / hour
- Tip element size ~ 330 nm
- Length scale, h = 2 nm
- Plotting atomic %, (lattice H)/Fe

Solving 5 fields simultaneously

Units are scaled in the balance of linear momentum, conservation of concentration, and L_2 projection to improve condition number of the system

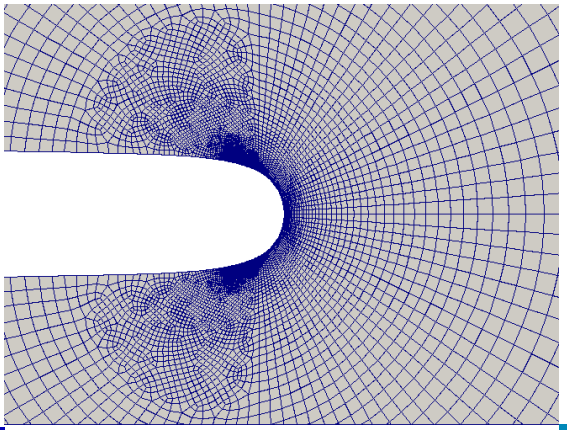

Because we have an analytical Jacobian, we employ Newton's method.

$$D^* \dot{C}_L$$

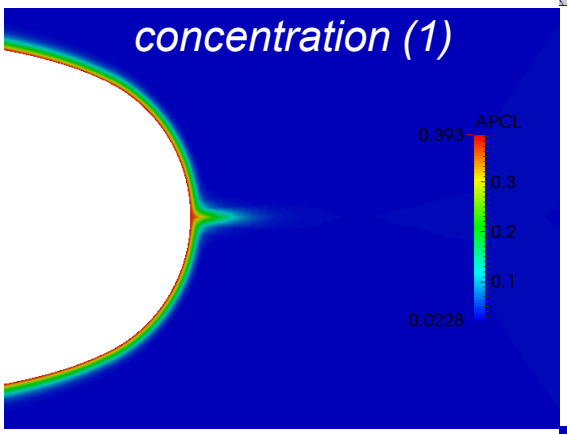

- Path: $10^2 D_0$
- K_{app}: 100 MPa $m^{1/2}$
- Time: 3600 s

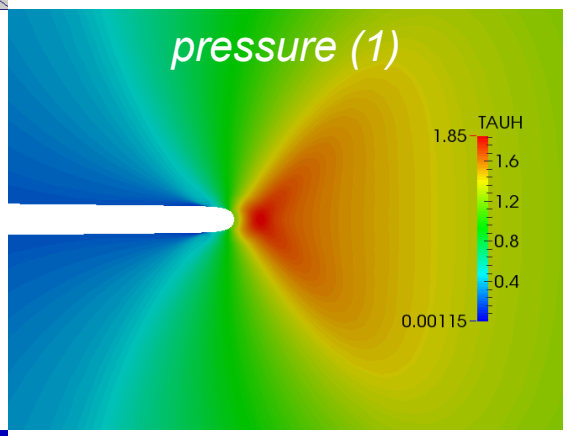

$$\nabla_{\boldsymbol{X}} \cdot d_l \boldsymbol{C}^{-1} \nabla_{\boldsymbol{X}} C_L$$

$$\nabla_{\boldsymbol{X}} \cdot \frac{d_l V_H}{RT} \boldsymbol{C}^{-1} \nabla_{\boldsymbol{X}} \tau_h C_L$$

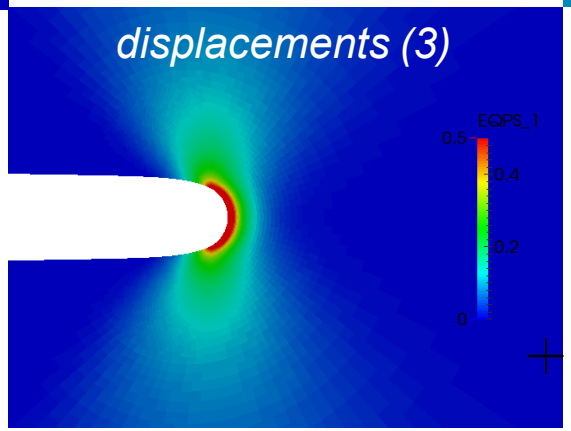

$$+ \theta_T \frac{dN_T}{d\epsilon_p} \dot{\epsilon}_p$$

NOTE: 100 MPa $m^{1/2}$ is well below J_Q for 21Cr-6Ni-9Mn (220 MPa $m^{1/2}$)

Natural sub-grid representation

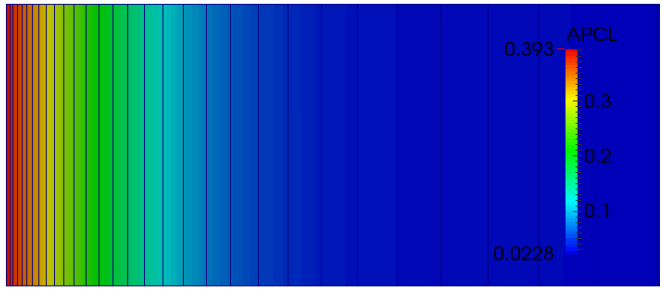

solution variables, C_L and τ_H

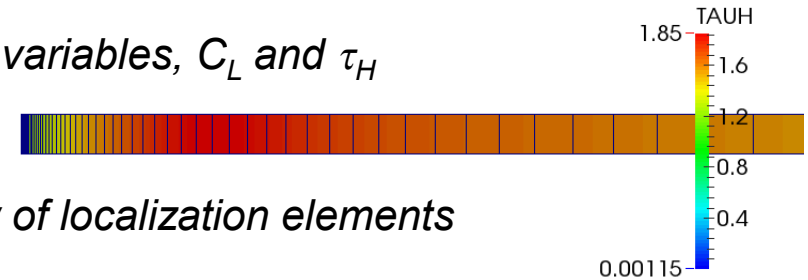

top view of localization elements

path: $10^2 D_0$, K_{app}: 100 MPa $m^{1/2}$, time: 3600 s

NOTE: Width of localization elements is 10 μm

Localization elements leverage bulk models

- Employing bulk, J_2 plasticity model
- Finite deformation kinematics
- Evolve stresses and internal state variables
- Employing bulk models for trapping
- Damage nucleation, growth straightforward

eqps

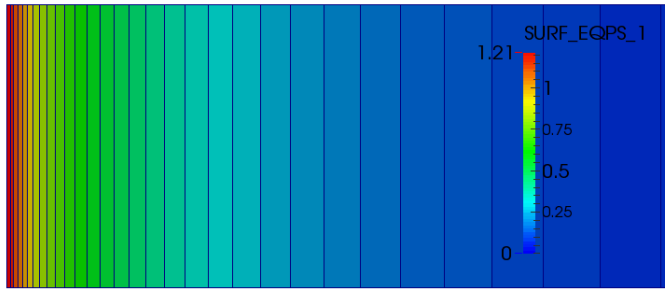

stress triaxiality

atomic % trapped hydrogen

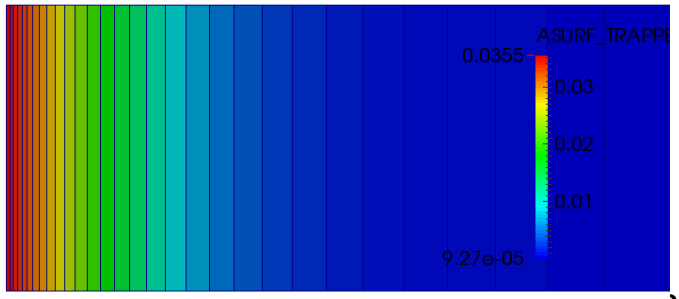

Future goal: Adaptive insertion along element boundaries (simplicial elements)

Summary and path forward

- Strong research environment
- Coupling is maturing
- Incorporated sub-grid multiphysics
- Enabled fast pathways
- Nucleation model maturing
- Propagation on horizon

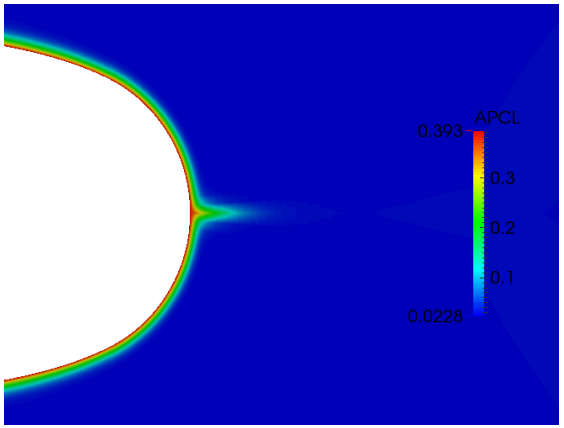

Our ability to form and test hypothesis through modeling and simulation can aid the discovery process and provide a pull for more fundamental measurements and computational methods.

Sandia National Laboratories

BACKUP SLIDES

Damage nucleation model w/H

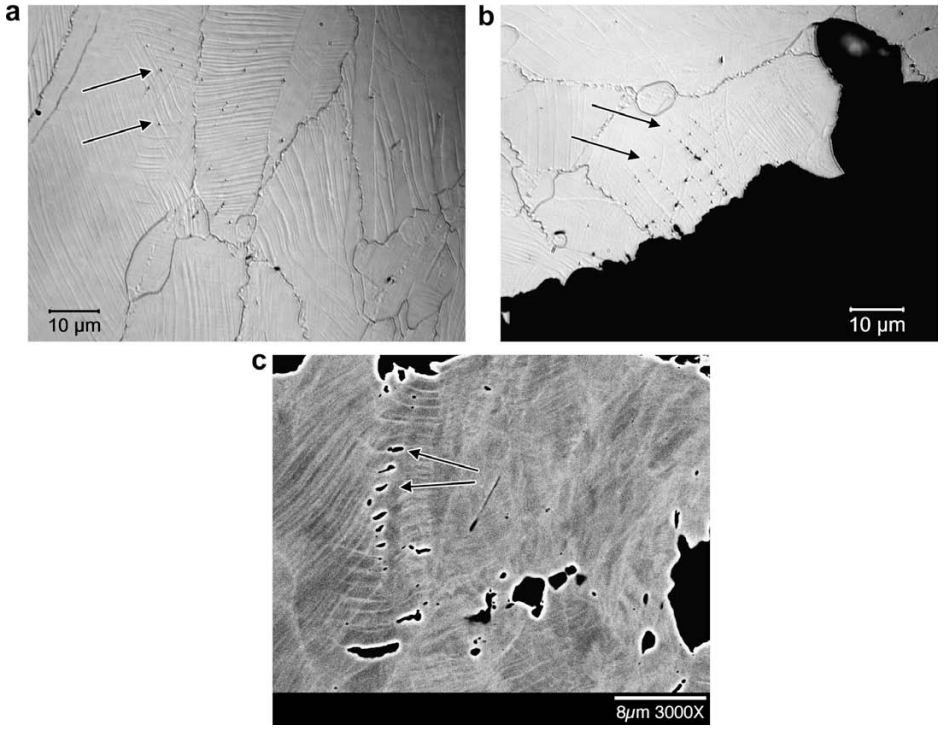

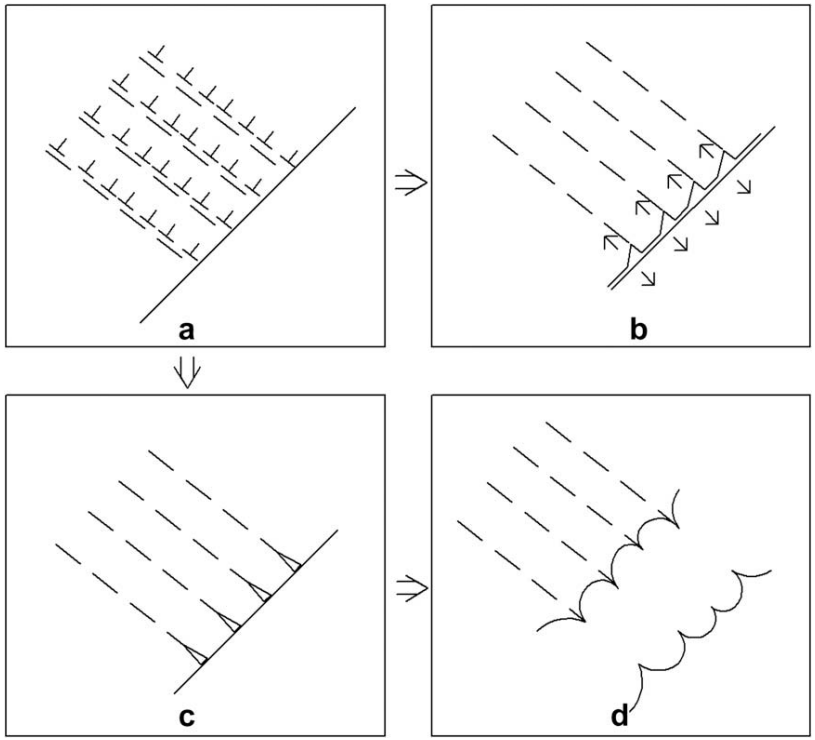

IDEA: Hydrogen enables the premature formation of planar deformation bands that impinge on boundaries of grains, annealing twins, and/or other deformation bands. The stress concentration induced by the intersection may nucleate a void of large aspect ratio (cylinder) that will evolve, coalesce and create the observed “fluted” fracture surface.

The fracture process is still ductile! Need to capture the premature nucleation of voids in the presence of hydrogen. Can we first construct a simple model to aid our intuition?

Analytical basis for nucleation

Stroh, A Theory of the Fracture of Metals, 1957

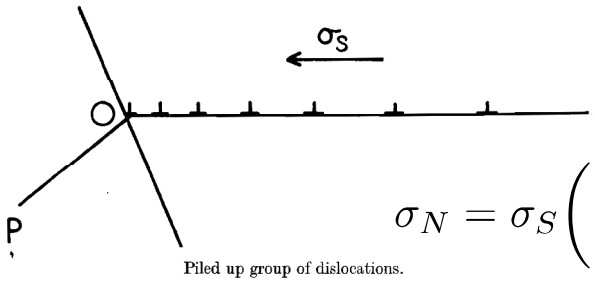

Piled up group of dislocations.

$$\sigma_N = \sigma_S \left(\frac{L}{r}\right)^{\frac{1}{2}} f(\theta)$$

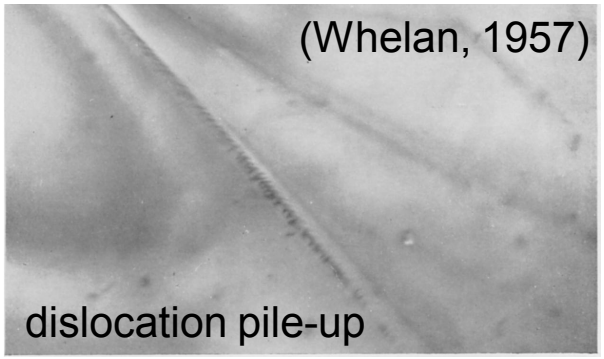

Using a work argument, the normal stress σ_N for nucleation can derived from the shear stress σ_S given the fracture energy γ and the number of dislocations *n* in a pile-up (band) along a boundary.

$$\sigma_{S,crit} = \frac{3\pi^2\gamma}{8n(\rho_{ss},\theta_T)b} \qquad n = A(\theta_T)\rho_{ss} = hs(\theta_T)\rho_{ss}$$

$$\kappa = \mu\epsilon_{ss}$$
$$\epsilon_{ss} = b\sqrt{\rho_{ss}}$$

Given *b* is burgers vector and *A* is an effective area characterized by the grain size *h* and the pile-up spacing *s*. We relate the pile-up spacing the to the occupancy of hydrogen in the traps θ_T. If we approximate σ_S through the yield stress σ_y and the isotropic hardening variable κ, we can express nucleation in terms of a scalar strain metric ε_{ss} that is reflective of the dislocation density ρ_{ss}.

$$\epsilon_{ss,crit}^3 + \frac{\sigma_y}{\mu}\epsilon_{ss,crit} - \frac{3\pi b\gamma}{4hs(\theta_T)\mu}$$

permits analytical solution (1 real root)

If we assume heavily worked materials, ρ_{ss} ~ 10^{15}, the specification of $s(\theta_T)$ becomes problematic. We need to construct a simplified model for nucleation in the correct state variable ε_{ss} that can capture a statistical sampling of boundary orientations having dislocation pile-ups (bands) which are stabilized and extended though hydrogen transport.

$$\theta_T = \frac{C_T}{N_T}$$

Occupancy of hydrogen in the traps θ_T derives from trapped concentration C_T and the number of traps N_T.

Phenomenological extension

The deformation bands that evolve under large deformations cannot be easily idealized

$$f_n = \frac{\phi_{n,0}}{\epsilon_{ss,std}\sqrt{2\pi}} \exp\left[-\frac{1}{2}\left(\frac{\epsilon_{ss}-\epsilon_{ss,mean}}{\epsilon_{ss,std}}\right)^2\right]$$

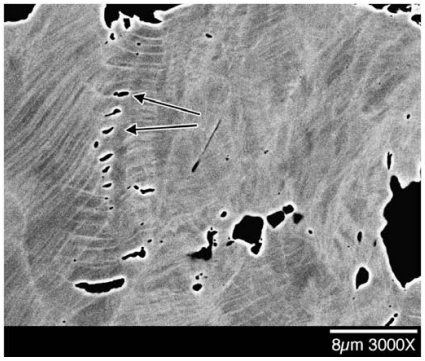

(Nibur, 2009)

In spirit of Chu and Needleman (1980) we choose an appropriate state variable to capture void nucleation through elevated stresses at pile-ups. We assume the probability of void nucleation f_n follows a normal distribution.

We assume that hydrogen affects the mean $\varepsilon_{ss,mean}$ and not the standard deviation $\varepsilon_{ss,std}$ through the occupancy of hydrogen in the traps θ_T. The nucleated void volume fraction ϕ_n can be found through integration and is limited by $\phi_{n,0}$.

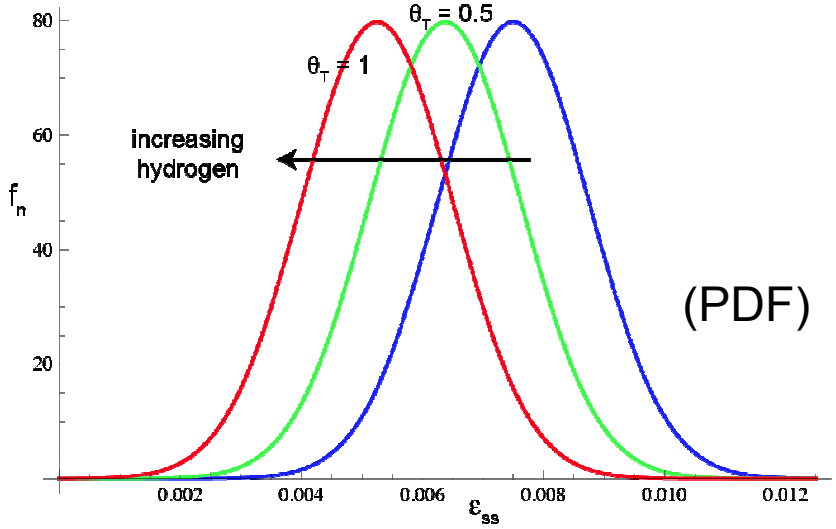

(PDF)

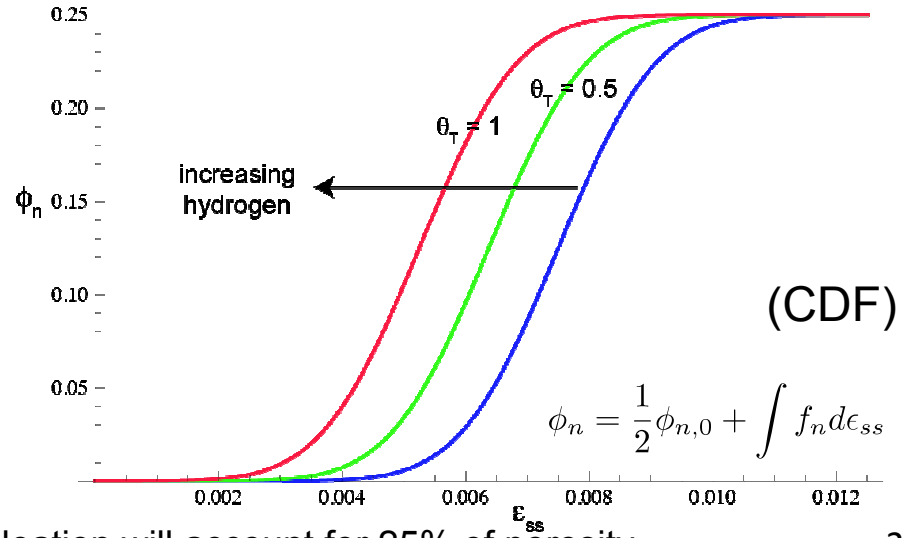

(CDF)

NOTE: In this case, we assume that $\phi_{n,0}$ is 0.25. Nucleation will account for 25% of porosity

Resolution required

r_p << L (150 mm) $2b_0$ (10 μm) << CTOD (155 μm)

undeformed, $2b_0$ = 10 μm

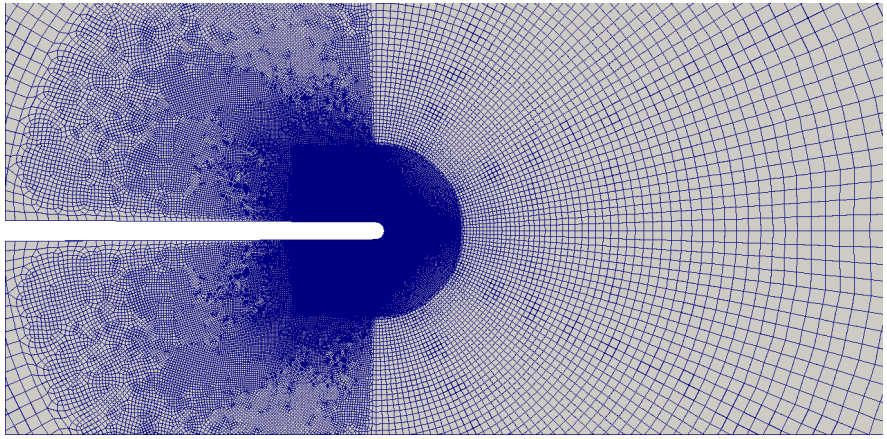

K = 50 MPa $m^{1/2}$, CTOD = 23.4 μm

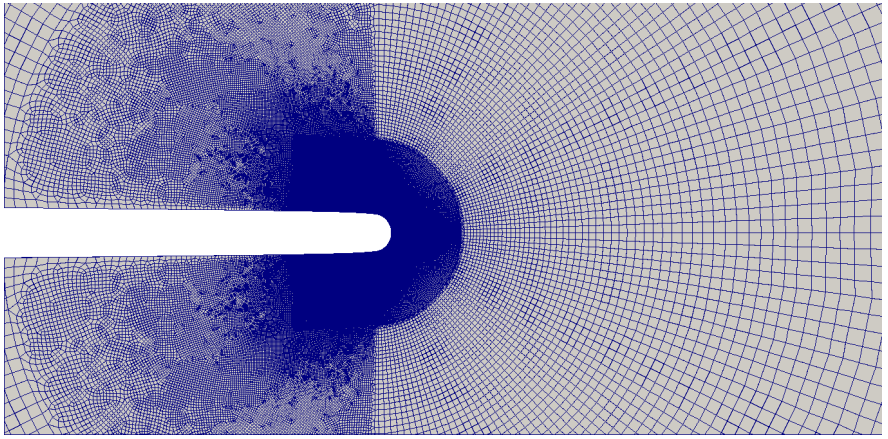

K = 110 MPa $m^{1/2}$, CTOD = 43.9 μm

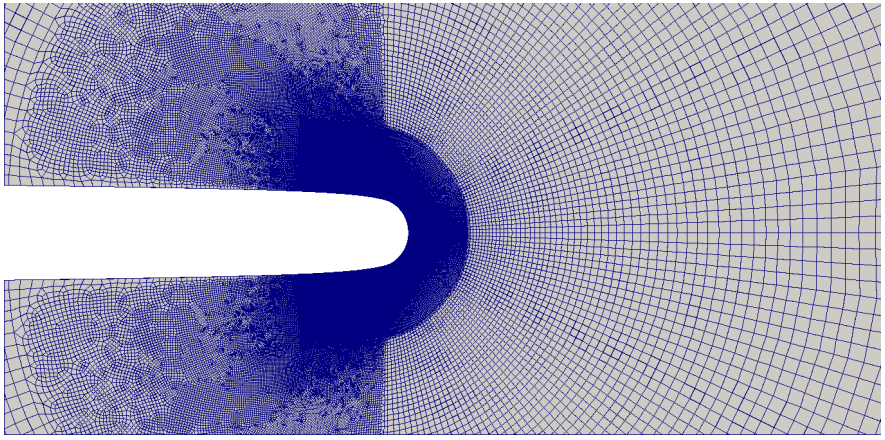

K = 220 MPa $m^{1/2}$, CTOD = 155 μm

We are required to resolve a diffusion front l_{front} that is ~ 0.5 μm, $CTOD_{max}/l_{front}$ ~ 310

Diffusion remains local and is resolved

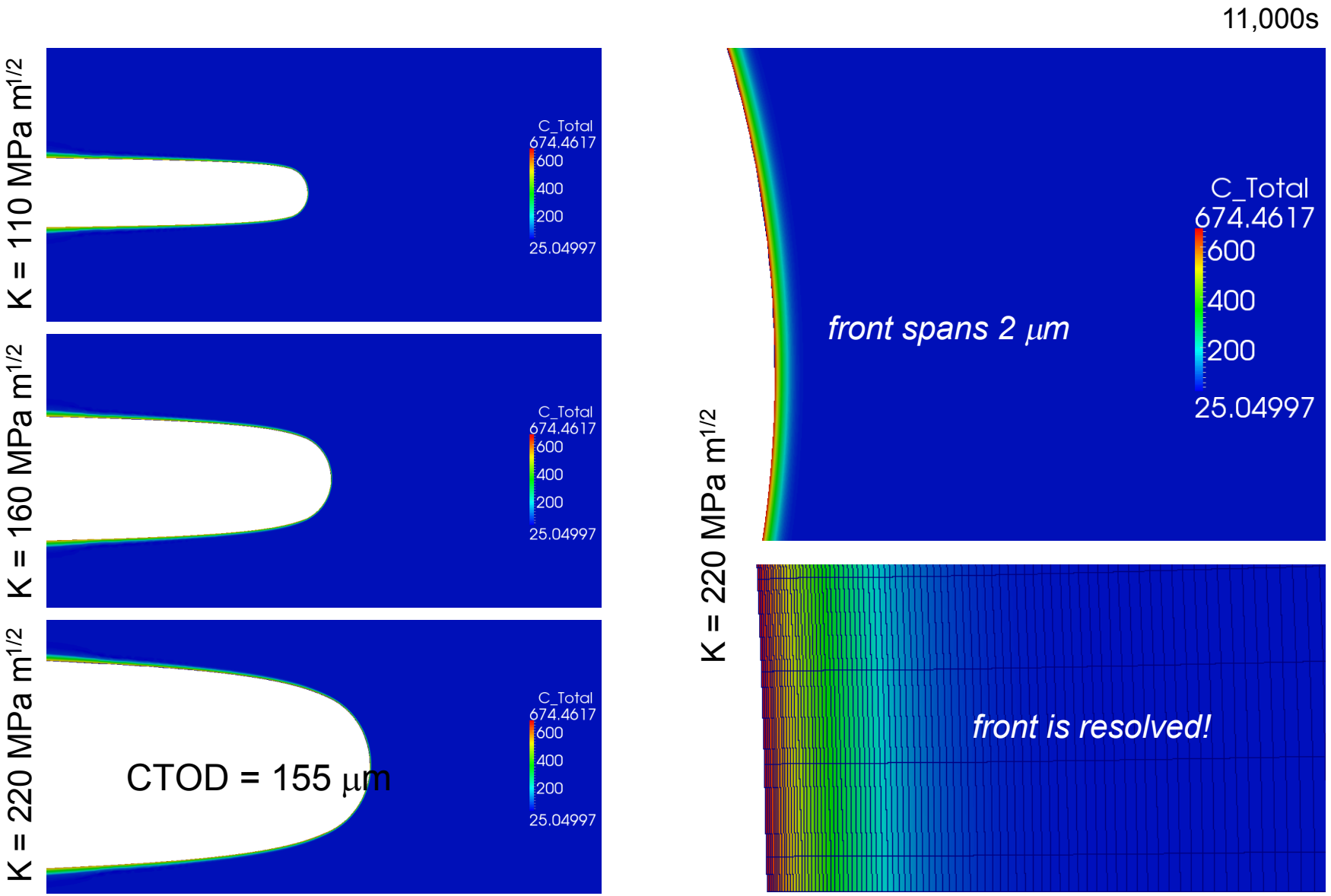

Increasing W_B compacts front

Increased binding energy W_B compacts front and substantially raises the total concentration

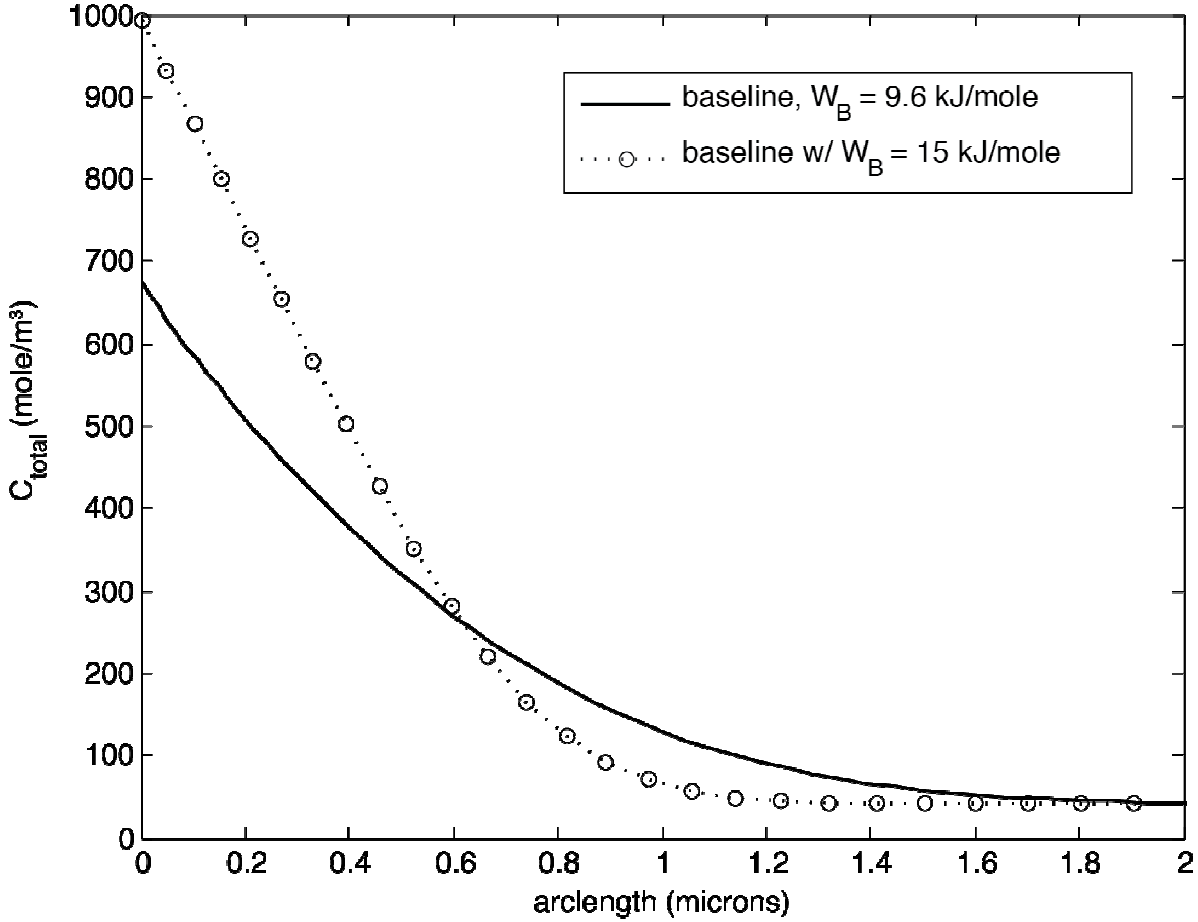

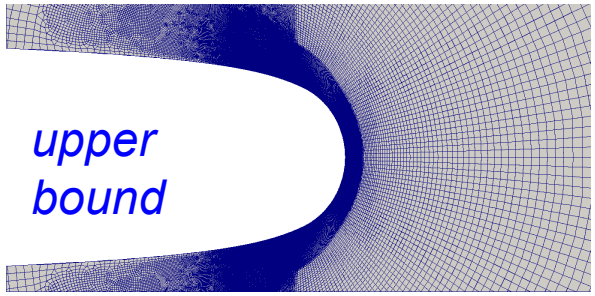

K = 220 MPa $m^{1/2}$
CTOD = 155 μm
time: 11,000 s

$$\theta_t = \frac{1}{1 + \frac{1}{k_t \theta_l}}$$

$$N_T = N_T(\epsilon_p)$$

$$k_t = e^{\frac{W_B}{RT}}$$

trapping

Diffusion front decreased by a factor of 2 – 2 μm to 1 μm
Total hydrogen concentration raised from 687 mol/m^3 to 991 mol/m^3

Faster loading rates compact front

- Test conditions: 1320 s and 13200 s to 220 MPa $m^{1/2}$
- Model cases: 688 s, 1375 s, 2750 s, 5500 s, and 11000 s to 220 MPa $m^{1/2}$
- Employing increased binding energy to investigate steeper gradients

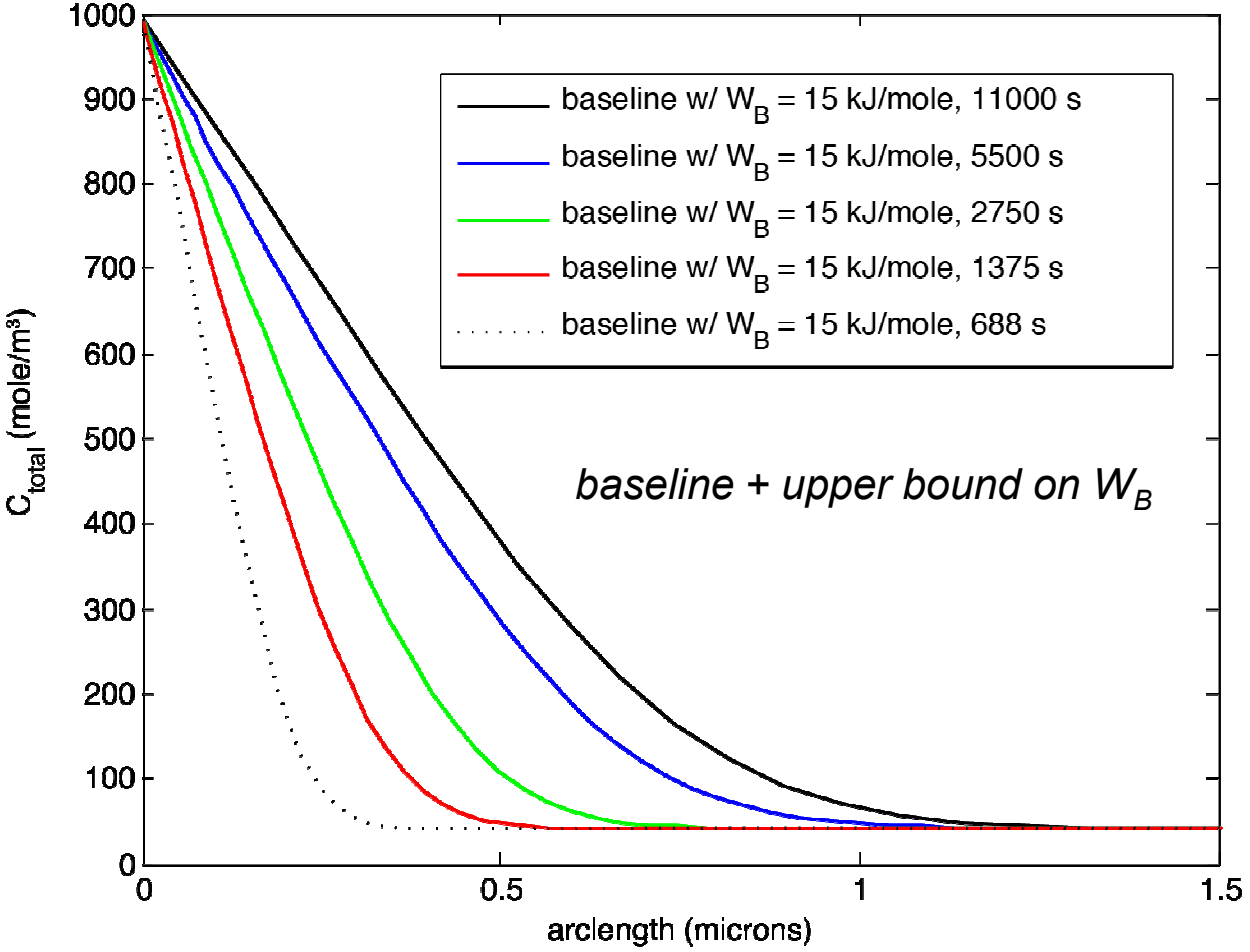

K = 220 MPa $m^{1/2}$
CTOD = 155 μm

More rapid loadings result in a diffusion front than spans only a few hundred nanometers.

Fast pathways or is this a surface effect?

Monolithic system for strong coupling

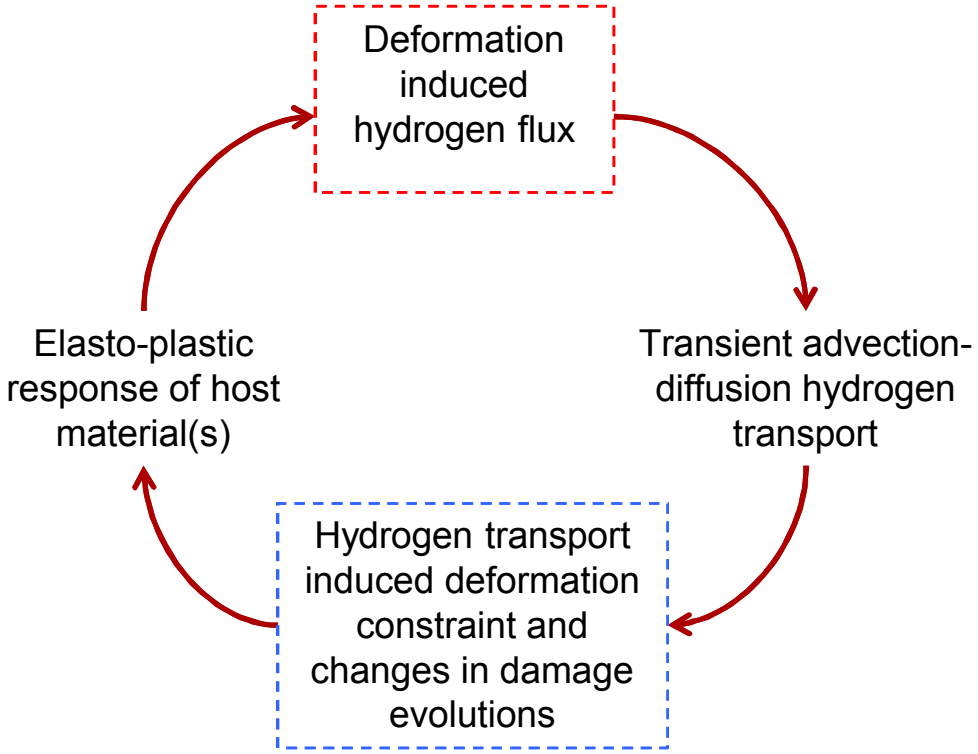

$$\begin{bmatrix} \mathbf{0} & \mathbf{0} \\ \boldsymbol{M}_{c_L u} & \boldsymbol{K}^{tran}_{c_L c_L} \end{bmatrix} \begin{bmatrix} \dot{\boldsymbol{u}} \\ \dot{\boldsymbol{c}}_{\boldsymbol{L}} \end{bmatrix} + \begin{bmatrix} \boldsymbol{K}_{uu} & \boldsymbol{B}_{uc_L} \\ \mathbf{0} & \boldsymbol{K}^{st}_{c_L c_L} \end{bmatrix} \begin{bmatrix} \boldsymbol{u} \\ \boldsymbol{c}_L \end{bmatrix} = \begin{bmatrix} \boldsymbol{F}^{ext}_{u} \\ \boldsymbol{F}^{ext}_{c_L} \end{bmatrix}$$

Physical interpretation of the matrix form

- When coupling terms (red and blue boxes) are **both** non-trivial, the coupling mechanism is two-way.
- There are two possible ways to solve two-way coupling problems are:
  - Iterative split-operator approach (Simo-Miehe 1992, Kim, Tchelepi and Juanes, 2013). In this case, solid mechanics and convection-diffusion solvers exchange information by allowing inconsistent linearization (i.e., freezing some nonlinear parameter, for instance, freezing displacement when solving for hydrogen concentration and vice versa) in each iteration.
  - Monolithic mixed finite element method, which guarantees consistency of the linearlization, but may lead to an ill-conditioned linearized system of equations (Sun, Ostien, Salinger 2013).